

Washington University in St. Louis

## Washington University Open Scholarship

---

Arts & Sciences Electronic Theses and  
Dissertations

Arts & Sciences

---


Winter 12-5-2018

# Synthesis and Integration of Oligoviologens into Hydrogel Actuators

Kevin Liles

*Washington University in St. Louis*

Follow this and additional works at: [https://openscholarship.wustl.edu/art\\_sci\\_etds](https://openscholarship.wustl.edu/art_sci_etds)

 Part of the [Materials Chemistry Commons](#), [Organic Chemistry Commons](#), and the [Polymer Chemistry Commons](#)

---

### Recommended Citation

Liles, Kevin, "Synthesis and Integration of Oligoviologens into Hydrogel Actuators" (2018). *Arts & Sciences Electronic Theses and Dissertations*. 1680.

[https://openscholarship.wustl.edu/art\\_sci\\_etds/1680](https://openscholarship.wustl.edu/art_sci_etds/1680)

This Thesis is brought to you for free and open access by the Arts & Sciences at Washington University Open Scholarship. It has been accepted for inclusion in Arts & Sciences Electronic Theses and Dissertations by an authorized administrator of Washington University Open Scholarship. For more information, please contact [digital@wumail.wustl.edu](mailto:digital@wumail.wustl.edu).

WASHINGTON UNIVERSITY IN ST. LOUIS

Department of Chemistry

Synthesis and Integration of Oligoviologens into Hydrogel Actuators

by

Kevin Patrick Liles

A thesis presented to the  
Graduate School  
of Washington University in  
partial fulfillment of the  
requirements for the degree  
of Master of Arts

December 2018  
St. Louis, Missouri

© 2018, Kevin Patrick Liles

# Table of Contents

List of Figures .....	iii
List of Tables.....	v
Acknowledgments.....	vi
Abstract.....	viii
Chapter 1: Introduction to Hydrogels.....	1
References.....	10
Chapter 2: Introduction to Viologens.....	12
References.....	24
Chapter 3: A Photoredox-Responsive Hydrogel Actuator .....	26
References.....	39
Chapter 4: A Redox-Responsive Reversible Phottopatterned Material Produced using Free- Radical Polymerization.....	42
References.....	50
Chapter 5: Concluding Remarks .....	51

# List of Figures

Figure 1.1: The different ways in which a polymer actuator (top) can behave, namely shrinking (left), twisting (bottom), and curling (right). .....	2
Figure 1.2: Image of the molecular motor (left) used to actuate a three dimensional network (right) in response to a UV wavelength light source. ....	4
Figure 1.3: Example of ionic polymer actuator with an ionic liquid encased in a poly(styrenesulphonate-b-methylbutylene) actuation in response to electrical stimuli .....	4
Figure 1.4: A box with PNIPAm joints can be folded and unfolded in response to temperature...5	5
Figure 1.5: Basic hydrogel properties.....8	8
Figure 1.6: The crossover point that occurs as a mixed epoxy resin hardens.....10	10
Figure 2.1: The three oxidation states of alkyl viologens.....12	12
Figure 2.2: Dilute methyl viologen in water is incapable of spin-pairing. Concentrated methyl viologen in water is a violet-purple color due to spin-pairing dimerization.....13	13
Figure 2.3: UV-Vis-NIR traces done of viologens reduced with sodium dithionite in water. a) Methyl viologen, no interaction; b) dimer viologen with 3-carbon tether; c) <i>ortho</i> -viologen dimer; d) <i>meta</i> -viologen dimer; and e) <i>para</i> -viologen dimer.....15	15
Figure 2.4: Schematic (left) and visual (far right) representations of the tris-radical inclusion complex of $MV^{•+} \subset CBPQT^{2(•+)}$ due to spin-pairing effects.....16	16
Figure 2.5: Schematic of the iterative synthesis of sequence-defined oligoviologens.....18	18
Figure 2.6: UV-Vis-NIR traces of oligoviologens of different lengths in (left) H <sub>2</sub> O and (right) MeCN.....19	19
Figure 2.7: Images of a viologen cube losing size and changing color as it reduces, followed by expansion and reoxidation in water .....	20
Figure 2.8: (Left) Rate of actuation of each hydrogel with 5 mol % oligoviologen incorporated and (Right) rate of actuation of mono-viologen-containing hydrogels with equivalent moles of viologen for each chain.....21	21
Figure 2.9: Comparison of the characteristics of a $6V^{12+}$ hydrogel between the contracted and swollen state using a frequency sweep at 1% strain amplitude.....22	22
Figure 2.10: Images of the $6V^{12+}$ cube performing work by lowering then lifting a dime.....23	23

Figure 3.1: The visual representation of the previous, chemically induced, hydrogel contraction .....	27
Figure 3.2: UV-Vis-NIR trace of $8V^{16+}$ Photoreduction.....	28
Figure 3.3: Experimental setup for blue-light irradiation.....	29
Figure 3.4: Kinetic data for each mol % of $8V^{16+}$ hydrogel.....	29
Figure 3.5: A) a table comparing the $G'$ of each contracted hydrogel after irradiation for five hours. B) a graph of the $G'$ value as a hydrogel is cycled through three contraction/expansion cycles.....	31
Figure 3.6: Images of the AMM as it undergoes work in response to a 450 nm light .....	33
Figure 3.7: Images of a 0 mol % viologen, i.e. 100 mol % PEG, hydrogel as it is irradiated for five hours with blue light. It is not capable of actuating, thus only undergoes dehydration.....	34
Figure 3.8: Emission spectrum of the ABI LED aquarium bulb used.....	36
Figure 3.9: Scheme for the synthesis of $8V-N_3 \bullet 16Tos$ .....	36
Figure 3.10: The rheological cycling of $8V^{16+}$ hydrogels .....	39
Figure 3.11: Damaged AMM after 5 hours of irradiation.....	40
Figure 4.1: Scheme for the integration of oligoviologen crosslinker into a HEA-based polymer network.....	43
Figure 4.2: Synthesis of $2V^{4+}$ -St.....	45
Figure 4.3: Photo patterning experimental setup.....	46
Figure 4.4: Kinetic plots of actuation out of total (a) and relative (b) volumes .....	47
Figure 4.5: Plot of frequency sweep from 0.1 to 100 rad s <sup>-1</sup> with strain set to 1%.....	49
Figure 4.6: Photo pattern disappearing from hydrogel as viologens are reoxidized and loose color. Yellow color is from ruthenium-based photocatalyst .....	49

# **List of Tables**

Table 2.1: Table indicating the moles of viologen per gel.....	19
Table 4.1: The amounts of each material used to fabricate viologen-containing hydrogels.....	45

# Acknowledgments

It must be said first to thank Dr. Jonathan Barnes, whose willingness to support and guide me during these two years of my graduate work cannot be overstated. Thanks must also be given to both Dr. John-Stephen Taylor, who was always available for questions regarding photocatalysis and for serving on my committee, and Dr. Julio D'Arcy, for his guidance and offer to help on a project concept, as well as serving on my committee. Everyone on my committee has been incredibly helpful and supportive to my growth as a scientist.

Thank you to the entirety of the J. Barnes group, both here and gone, for being supportive during my graduate work. Special thanks must be given to Dr. Angelique Greene, without whom the initial viologen work would not have been accomplished. I also need to thank Nate Colley, Abigail Delawder, and Dr. Faheem Solangi, each of whom has worked with me on a viologen project in some shape or form.

It would be remiss of me to not thank my family, especially my parents Kelly and Karen, who have always been there for me throughout my many years away from home. But truly, the most thanks must go to Marina Davis, for her endless emotional support through the result-less days and weeks. I'm eternally grateful that I can be yours.

Kevin P. Liles

*Washington University in St. Louis*

*December 2018*



*To my love*

## ABSTRACT OF THE THESIS

Synthesis and Integration of Oligoviologens into Hydrogel Actuators

by

Kevin Patrick Liles

Master of Arts

Chemistry

Washington University in St. Louis, 2018

Professor Jonathan Barnes, Chair

Interest in the development of soft-material artificial molecular muscles has inspired scientists to pursue novel stimuli-responsive systems capable of undergoing change in the physical and mechanical properties of a material in response to external stimuli. This interest has been driven primarily by advances, or the desire for advances, in fields such as soft robotics, microfluidics, and bio-compatible drug-delivery systems. In this work, redox-responsive viologens and their ability to form stable radical-cation complexes were evaluated as a method of actuation in stimuli-responsive materials, specifically hydrogels.

First, a brief overview of hydrogel actuators is covered, with some examples given of the broad varieties of stimuli-responsive hydrogels. Then, viologens and their behavior and characteristics are discussed, with special attention paid to the effect of the tether between viologens on their ability to pimerize and the previous work on incorporating viologens into hydrogel actuators.

A study was performed to allow viologen-containing hydrogels to respond to a different stimuli than was implemented previously, namely the use of light to actuate the viologen-

containing hydrogel using a blue light sensitive photo-redox catalyst that allowed the material to lose 50% of its total volume over five hours. In the same study, it was also shown that the integration of oligoviologen above 5 mol % was detrimental to the physical properties of the material with no noticeable benefit in actuation speed or amount.

Viologen-containing hydrogels were then incorporated into a hydrogel network using a different method of polymerization, namely uncontrolled free radical polymerization where the previous studies had utilized copper-mediated azide-alkyne “click” chemistry. These hydrogels were shown to actuate in a similar manner and change color to those shown in previous studies. These viologen-containing hydrogels were then photopatterned using a mask and a ruthenium-based photocatalyst. There is a lot of potential for these viologens to be utilized in hydrogel actuators due to their responsiveness to differing stimuli, such as those described here.

# **Chapter 1: Introduction to Hydrogels**

Soft materials are a class of materials that are capable of being easily deformed at room temperature.<sup>2</sup> Soft materials as a class include, but are not limited to, foams, gels, ionic liquids, elastomeric plastics, and soft biological materials such as organ or muscle tissue. Soft materials are the opposite of hard materials, which typically require elevated temperature or excessive force to deform, such as most metals or crystals.<sup>21</sup>

## **1.1 Interest in Soft Materials**

Soft materials have drawn increasing interest in areas where traditional hard materials are not easily applicable. Researchers attracted to soft materials are those working with biological systems, self-healing materials, soft robotics, and at micro- or nanometer, scales. Many polymers, such as poly(ethylene glycol) (PEG) or poly(dimethylsiloxane) (PDMS), are flexible enough to allow integration into biological systems, making them of particular interest in semi-permanent, slow-releasing drug systems.<sup>13</sup> Soft robotics are designed to be capable of great behavioral diversity, whereas traditional, hard, robotics are intended to do a single action well, similar to the differences between human muscle and a motor.<sup>4</sup>

## **1.2 Hydrogel Actuators**

Hydrogels are a subclass of soft materials composed of a three-dimensional polymer network swollen with water, where the aqueous phase makes up 95–99 weight percent of the swollen material.<sup>1</sup> Organogels are a separate but related subclass of soft materials, where instead of water a polymer network is instead swollen with a typically polar, organic solvent such as dimethylformamide (DMF) or acetonitrile (MeCN). The capability of a particular hydrogel network to swell is determined by a number of factors – such as the crosslinking density of the

network, as water fills the space between network chains – and the hydrophilicity of the monomers used to create the network, as water undergoes hydrogen bonding with polar hydrophilic groups.<sup>14</sup> The higher the crosslinking density of a given polymer network, the smaller the pore size and the less water that can fit in those pores, in addition to less expansion of polymer chains. The hydrophilicity of the monomeric units used to create the network will carry over, with increasing hydrophilicity resulting in a greater amount of network swelling.

Hydrogels are effective actuators due to their large water content, which allows for large degrees of actuation, i.e., shrinking and swelling, as water leaves the polymer system in response to an external stimulus. The types of stimuli used to actuate soft materials includes, but is not limited to: (i) irradiation with light,<sup>9-10</sup> (ii) electrochemical activation,<sup>17,19,22</sup> and (iii) changes in temperature,<sup>5,6</sup> or (iv) pH.<sup>18,23</sup> Many of these methods are used to indirectly change either the crosslinking density, pore size, or hydrophilicity, resulting in swelling or shrinking of the polymer network (Fig 1.1).<sup>15</sup>

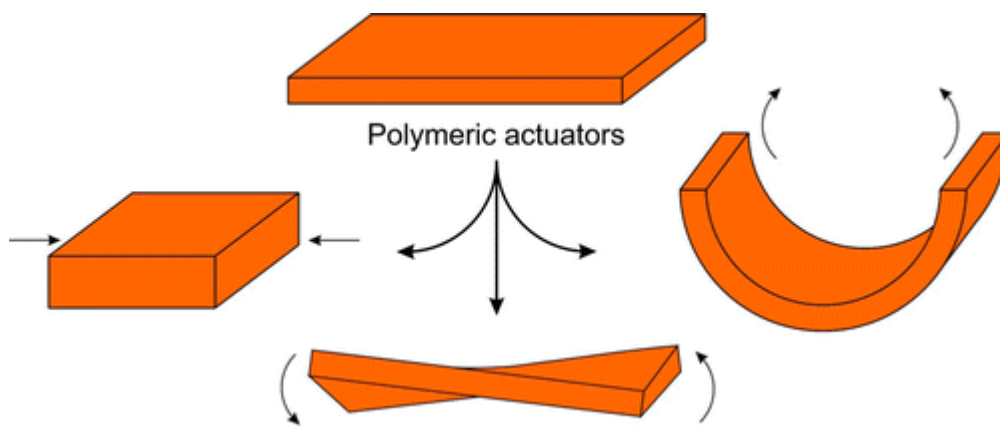


Figure 1.1 The different ways in which a polymer actuator (top) can behave, namely shrinking (left), twisting (bottom), and curling (right). Replicated with permission from ref [15].

### 1.2.1 Photo-Responsive Actuators

One example of a photo-responsive hydrogel actuator is the work of Harada and co-workers utilizing the host-guest complex of  $\alpha$ -cyclodextrin ( $\alpha$ CD) and azobenzene.<sup>9-10</sup>  $\alpha$ CD and an azobenzene derivative were incorporated into a polymer network as pendant groups “hanging” off the polymers comprising the network.<sup>10</sup> Under ambient conditions, the azobenzene is in the *cis* configuration, allowing complexation since the *trans*-azobenzene can fit inside the cavity of the  $\alpha$ CD. In this configuration, the polymer network has additional crosslinking junctions, causing the network to be more tightly bound together and possessing a lower water content. UV light converts the complexed *trans*-azobenzene to *cis*, which leads to decomplexation and swelling as the *cis*-azobenzene can no longer fit inside the  $\alpha$ CD. This process is fully reversible, with irradiation by visible light leading to the *cis* to *trans* isomerization, causing the  $\alpha$ CD/azobenzene complex to reform and shrink the material. This and similar host-guest complex approaches have been used to actuate hydrogels using a variety of stimuli such as switchable redox states and photoisomerization.<sup>24,25</sup>

A less conventional, but no less effective, example of light-activated hydrogel actuators is the work of Giuseppone and co-workers incorporated small molecular motors, sometimes known as Feringa motors, into the crosslinking junctions of hydrogel networks (Fig. 1.2).<sup>12</sup> These molecular motors rapidly isomerize when exposed to UV light. As the motor rotates, it causes the network to become entangled and the material to shrink. They later added a method by which the network can be unwound, allowing full cycling of the material.<sup>11</sup>

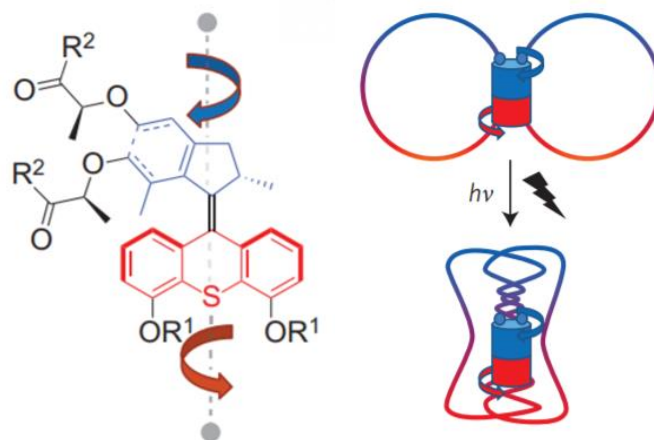


Figure 1.2 Image of the molecular motor (left) used to actuate a three dimensional network (right) in response to a UV wavelength light source. Replicated with permission from ref. [12].

## 1.2.2 Electrochemical Actuators

Electrochemical actuators are materials that are responsive to electric fields. Though the method of actuation is the same, there are a wide variety of mechanisms for this to occur by. One example is ionic polymer actuators.<sup>16</sup> These are typically ionic liquids, poorly coordinated liquid salts, encased in a flexible polymer casing. Upon application of an electrical current, the highly mobile cations in the ionic liquid will migrate to the cathode, causing the material to bend due to the cathode side swelling and the anode side shrinking as the fluid moves through the material (Fig. 1.3).

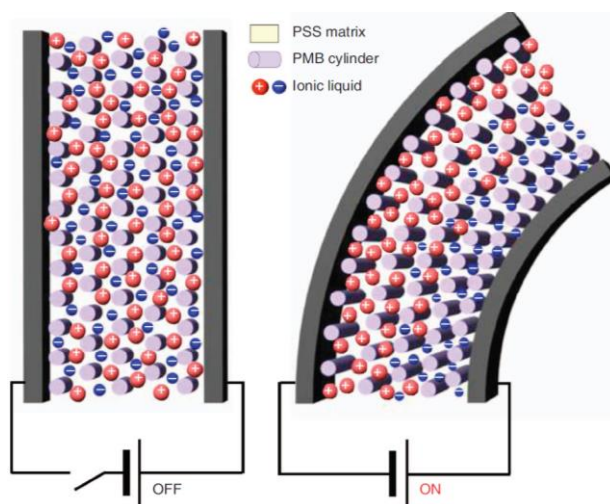


Figure 1.3 Example of ionic polymer actuator with an ionic liquid encased in a poly(styrenesulphonate-b-methylbutylene) actuation in response to electrical stimuli. Reprinted with permission from ref. [16].

Another example takes advantage of the redox-responsive properties of ferrocene to modify the crosslinking density of a hydrogel.<sup>17</sup> Neutral ferrocene is capable of fitting inside the cavity of  $\beta$ CD, whereas the oxidized, positive, ferrocene will disassociate from the complex. This supramolecular complex was implemented by Yuan and co-workers to create a material that was a gel, crosslinked by this ferrocene/CD complex, which upon oxidation at 1.0 V causes a gel-to-sol transition. The gel can be reformed by exposing the sol to heat, reestablishing the hydrogel network.

### 1.2.3 Temperature-Responsive Actuators

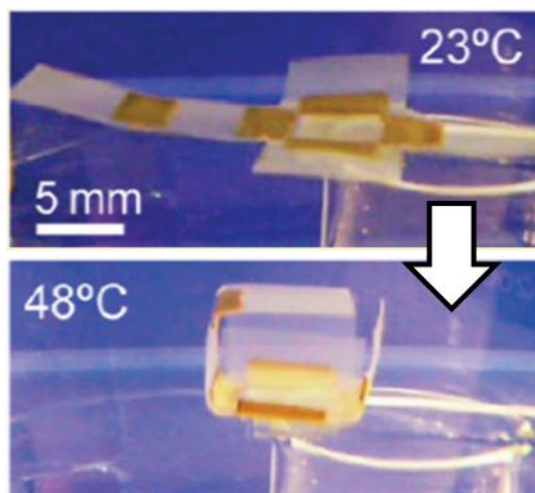


Figure 1.4 A box with PNIPAm joints can be folded and unfolded in response to temperature. Copied with permission from [6].

Hydrogels composed of poly(*N*-isopropylacrylamide) (PNIPAm) are an example of a thermos-responsive hydrogel, which actuate in response to changes in temperature (Fig 1.4).<sup>5,6</sup> These PNIPAm-based gels are typically synthesized via free-radical polymerization with a crosslinker such as methylenebis(acrylamide) to form the necessary three-dimensional network, with PNIPAm being the majority component with little or no other monomers.<sup>8</sup> At temperatures below 32°C, PNIPAm hydrogen bonds with water, forming an ordered structure and allowing for retention of water inside the pores of the network. Upon heating the hydrogel above 32°C,



however, the increased entropy caused by the temperature overwhelms the enthalpic hydrogen bonding contribution and forces the release of most of the water in the system. This release causes a large degree of actuation of the hydrogel and can take less than a minute. While this seems like an ideal material, PNIPAm-based gels are extremely fragile and usually require adherence to a more sturdy and robust material during practical applications.<sup>3,7</sup>

#### **1.2.4 pH-Responsive Actuators**

Hydrogels that respond to pH can be capable of great degrees of actuation, usually by modifying the hydrophilicity of the network. Nanocomposite hydrogels composed of hybridized poly-vinyl alcohol (PVA) and ferritin nanoparticles are one example of a pH-responsive actuator.<sup>18</sup> A nanocomposite hydrogel is one that is composed of a traditionally crosslinked network doped with additive nanoparticles or sometimes biological proteins or enzymes. In this example, ferritin is capable of forming networks due to the carboxylic acid and amine groups on the ferritin protein. Not only does this protein form additional crosslinks, thereby strengthening the mechanical properties of the material, but it also causes pH responsiveness. The ferritin-containing gels swell in response to basic pH. This is due to the ferritin protein microfibers expanding, increasing the pore size of the material and facilitating movement and absorption of water into the hydrogel network.

### **1.3 Hydrogel Characterization**

Desired properties in hydrogel actuators include: a fast rate of actuation in both shrinking and swelling, large degrees of actuation, and strong mechanical properties. All of these relate back to the ability of a particular hydrogel to do work, with the rate of actuation determining how fast the hydrogel is capable of functioning, degrees of actuation determining the amount of work that can

be done, and strong mechanical properties to work under more stringent conditions and move heavier loads than a comparatively weaker material.

### **1.3.1 Rate and Degree of Actuation**

The rate of actuation is easily determined using a couple of differing methods. The first is to measure the physical dimensions of the hydrogel to determine its volume. Though the easiest, this method can be difficult for those with non-uniform shapes. Another way to measure actuation is to take the weight of the hydrogel during actuation, as its weight should lower as water is removed from the network or vice versa.<sup>20</sup> Measuring the weight of the hydrogel during actuation is not viable for those that rely on chemical additives during actuation as the fluctuation of ions or salts will affect the weight of the hydrogel. Ionic polymer actuators, instead, are typically measured using displacement, as they do not change size or weight as they actuate.<sup>15,19</sup>

The degree of actuation is determined as the percentage of the final volume, or displacement, divided by the initial, and is therefore measured in the same method as rate of actuation, with the size of the material being actuated playing the largest role. Varying methods of actuation, light, heat, etc., have different rates of actuation. Electrical means of actuation is typically the fastest method of actuation, where small, thin ionic polymer actuators are capable of oscillating up to hundreds of times a second, others are far slower, with photochemical actuation often taking hours, and occasionally days, to fully contract.<sup>1, 16</sup> These rates are considering the material being actuated as approximately the same size. Electrical contraction can take minutes at the large, centimeter scale, while light can function in seconds on a millimeter-sized material.

### 1.3.2 Mechanical Properties

The mechanical properties of soft materials can be measured in a number of ways, such as tension and compression testing, indentation with a probe, or a frequency-based test such as shear rheometry or dynamic mechanical analysis. In the work described in chapter 3 and 4, shear oscillatory rheology was used, which can be understood in terms of storage ( $G'$ ) and loss ( $G''$ ) moduli.<sup>2</sup> The  $G'$  is also referred to as the shear elastic portion, and the  $G''$  the shear viscous portion. Both are measured in Pascals (Pa) and can be used to find the complex shear modulus, ( $G^*$ ) in the following formula, where  $i$  is the imaginary number.

$$G^* = G' + iG''$$

These storage and loss moduli are heavily related to other intrinsic aspects of a hydrogel material, such as the crosslinking density ( $\rho_x$ ), the water content of a hydrogel ( $Q$ ), the mesh size of the network ( $\zeta$ ), the rate of diffusion of molecules and through the network ( $D$ ), and the gel mechanics, such as ( $G$ ) and other related terms such as  $G'$ . None of these factors can be changed without affecting the others; as the mesh size  $\zeta$  increases, the rate of diffusion and water content increase, while the storage modulus  $G'$  decreases (Fig. 1.5).<sup>27</sup>

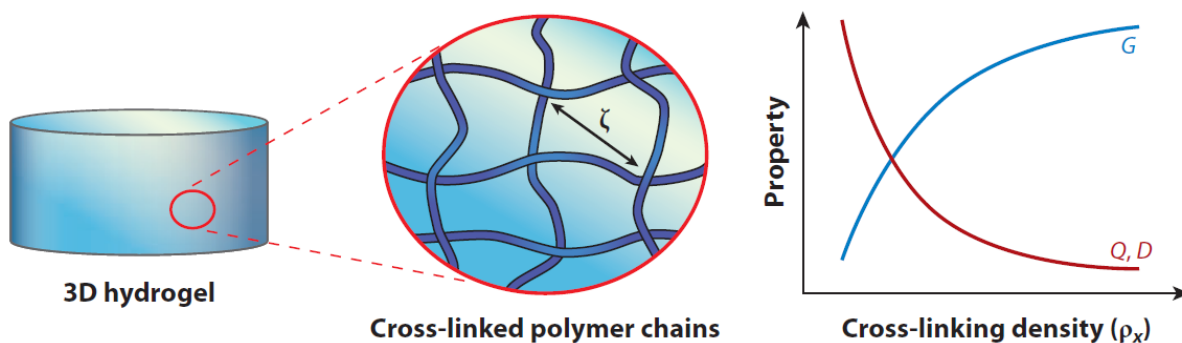


Figure 1.5: Basic hydrogel properties. Reprinted with permission from ref [27].

When the  $G'$  is a greater value than  $G''$ , the material behaves in a solid-like manner. This means that any energy absorbed by the material, such as friction due to oscillation, is stored by stretching of the internal structure. This energy can then later be used to reform the previous shape of the material after it is released. This property is what allows some elastomeric materials to distort their shape up to 1000% elongation while maintaining full reversibility. Most hydrogels display this behavior in the swollen state.

Viscoelastic liquids with  $G''$  greater than  $G'$ , however, have a larger loss modulus. This indicates that there is no strong internal structure, and energy is lost through internal friction and is not available to reform the material after the deformation force is removed.

These rheological values are not static, and will potentially undergo a crossover point, which is the shear rate, or force, which when applied causes  $G'$  to overtake  $G''$  or vice versa. This can happen in a variety of scenarios.  $G''$  can overtake  $G'$  in regards to hydrogels if, for example, the material undergoes a gel-sol transition such as in the example with the gel crosslinked with  $\beta$ CD and ferrocene mentioned in 1.2.2.<sup>17</sup> As the crosslinking junctions begin to disassociate, the  $G'$  value falls while the  $G''$  value rises, until ultimately the  $G''$  becomes greater, causing a crossover point, and the time at which the gel completely dissolves into a solution. The opposite can also be seen, with the pre-gel solution beginning to solidify as crosslinking junctions are formed, with the gel completely forming at the crossover point (Fig. 1.6).<sup>26</sup>

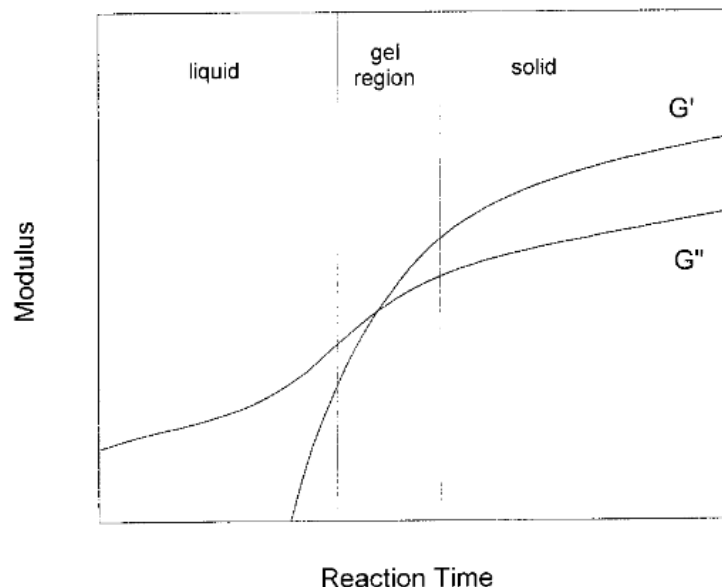


Figure 1.6: The crossover point that occurs as a mixed epoxy resin hardens. Reprinted with permission from Ref. [26]

## References: Chapter 1

1. Ionovo, L. Hydrogel-based actuators: possibilities and limitations. *Mater. Today*. **2014**, *17* (10), 494–503.
2. Sollich, P., Lequeux, F., Hébraud, P., and Cates, M. E. Rheology of Soft Glassy Materials. *Phys. Rev. Lett.* **1997**, *78*, 2020
3. Delaney, C., McCluskey, P., Coleman, S., Whyte, J., Kent, N., Diamond, D. Precision control of flow rate in microfluidic channels using photoresponsive soft polymer actuators. *Lab Chip*, **2017**, *17*, 2013–2021
4. Alici, G. What Differentiates Soft Robotics from Hard Robotics?. *MRS Advances*. **2018**, *3*, 1557–1568
5. Haq, M.A., Su, Y., Wang, D. Mechanical properties of PNIPAm based hydrogels: A review. *Mater. Sci. Eng. C*. **2017**, *70*, 842–855.
6. Zhang, X. et. al. Optically- and Thermally-Responsive Programmable Materials Based on Carbon Nanotube-Hydrogel Polymer Composites. *Nano Lett*, **2011**, *11*, 3239–3244.
7. Li, X., Cai, X., Gao, Y., Serpe, M.J. Reversible bidirectional bending of hydrogel-based bilayer actuators. *J. Mater. Chem. B*. **2017**, *5*, 2804–2812
8. Kim, D., Lee, H.S., Yoon, J. Highly bendable bilayer-type photo-actuators comprising of reduced graphene oxide dispersed in hydrogels. *Sci. Rep.* **2016**, *6*, 1–10.
9. Nakahata, M., Takashima, Y., Hashidzume, A., Harada, A. Redox-Generated Mechanical Motion of a Supramolecular Polymeric Actuator Based on Host-Guest Interactions. *Angew. Chem. Int. Ed.* **2013**, *52*, 5731–5735.
10. Takashima, Y., Hatanaka, S., Otsubo, M., Nakahata, M., Kakuta, T., Hashidzume, A., Yamaguchi, H., Harada, A. Expansion-contraction of photoresponsive artificial muscle regulated by host-guest interactions. *Nat. Commun.* **2012**, *3*:1270 doi: 10.1038/ncomms2280

11. Foy, J.T., Li, Q., Goujon, A. Colard-Itte, J. R., Fuks, G., Moulin, E., Schiffmann, O., Dattler, D. Funeriu, D. P., Giuseppone, N. Dual-light control of nanomachines that integrate motor and modulator subunits. *Nat. Nanotechnol.*, **2017**, *12* (6), 540–545
12. Li, Q., Fuks, G., Moulin, E., Maaloum, M., Rawiso, M., Kulic, I., Foy, J. T., Giuseppone, N. Macroscopic contraction of a gel induced by the integrated motion of light-driven molecular motors. *Nat. Nanotechnol.* **2015**, *10*, 161–165.
13. *Highlights of prescribing information* [Webpage] [cited 25 November 2018], Merck PDF detailing all relevant information on the hormonal implant NEXPLANON]. Available from [https://www.merck.com/product/usa/pi\\_circulars/n/nexplanon/nexplanon\\_pi.pdf](https://www.merck.com/product/usa/pi_circulars/n/nexplanon/nexplanon_pi.pdf)
14. Hoffman, A. S. Hydrogels for biomedical applications. *Adv. Drug Deliver Rev.*, **2002**, *54*, 3–12.
15. Ionovo, L. Polymeric Actuators *Langmuir*, **2015**, *31*, 5015–5024.
16. Kim, O., Shin, T. J., Park, M. J. Fast low-voltage electroactive actuators using nanostructured polymer electrolytes. *Nat. Commun.* **2013**, *4*, 2208.
17. Nakahata, M., Takashima, Y., Yamaguchi, H., Harada, A. Redox-responsive self-healing materials from host-guest polymers. *Nat. Commun.* **2011**, *2*, 511.
18. Shin, M. K., Spinks, G. M., Shin, S. R., Kim, S. I., Kim, S. J. Nanocomposite Hydrogel with High Toughness for Bioactuators. *Adv. Mater.* **2009**, *21*, 1712–1715.
19. Bronchu, P., Pei, Q. Advances in Dielectric Elastomers for Actuators and Artificial Muscles. *Macromol. Rapid Commun.* **2010**, *31*, 10–36.
20. Wang, B., Tahara, H., Sagara, T. Driving Quick and Large Amplitude Contraction of Viologen-Incorporated Poly-L-Lysine-Based Hydrogel by Reduction. *ACS Appl. Mater. Interfaces*, **2018**, *10*, 36415–36424.
21. *What is Creep* [Webpage] [cited 25 November 2018], Defining creep in terms of permanent deformation of hard materials. Available from <http://www.diecastingdesign.org/thermal-creep>
22. Pelrine, R., Kornbluh, R., Pei, Q., Joseph, J. High-Speed Electrically Actuated Elastomers with Strain Greater than 100%. *Science* **2000**, *287*, 836–836
23. Azrzar, L. D., Kim, P., Aizenberg, J. Bio-inspired Design of Submerged Hydrogel-Actuated Polymer Microstructures Operating in Response to pH. *Zdv. Mater.* **2011**, *23*, 1442–1446.
24. Kakuta, T. et al., Preorganized Hydrogel: Self-Healing Properties of Supramolecular Hydrogels Formed by Polymerization of Host-Guest-Monomers that Contain Cyclodesxtrins and Hydrophobic Guest Groups. *Adv. Mater.* **2013**, *25*, 5849–2853.
25. Appel, E. A. et al. Supramolecular Cross-Linked Networks *via* Host-Guest Complexation with Cucurbit[8]uril. *J. Am. Chem. Soc.* **2010**, *132* (40), 14251–14260.
26. Mortimer, S., Ryan, A. J., Stanford, J. L. Rheological Behavior and Gel-Point Determination for a Model Lewis Acid-Initiated Chain Growth Epoxy Resin. *Macromolecules.* **2001**, *34*, 2973–2980.
27. DeForest, C. A., Anseth, K. S. Advances in Bioactive Hydrogels to Probe and Direct Cell Fate. *Annu. Rev. Chem. Biomol. Eng.* **2012**, *3*, 421–444.

# Chapter 2: Introduction to Viologens

Parts of this chapter, notably section 2.3, is partially based on work described in the following publication: Greene, A. F.; Danielson, M. K.; Delawder, A. O.; Liles, K. P.; Li, X.; Natraj, A.; Wellen, A.; Barnes, J. C.: Redox-Responsive Artificial Molecular Muscles: Reversible Radical-Based Self-Assembly for Actuating Hydrogels. *Chem Mater.*, **2017**, 29 (21), 9498-9508.<sup>17</sup>

Viologens<sup>1</sup> are a class of redox-active materials consisting of 1,1'-dialkyl-4,4'-bipyridinium moieties (i.e., alkyl viologens).<sup>2</sup> For example, 1,1'-dimethyl-4,4'-bipyridinium is commonly referred to as “methyl viologen,” just as 1,1'-dibenzyl-4,4'-bipyridinium is “benzyl viologen.” Much of the interest in viologens stems from their variable oxidation states (Fig 2.1) and self-assembly properties, most notably supramolecular complexes<sup>5,6</sup> and radical molecular self-recognition.<sup>3,4</sup>

## 2.1 Oxidation States of Viologens

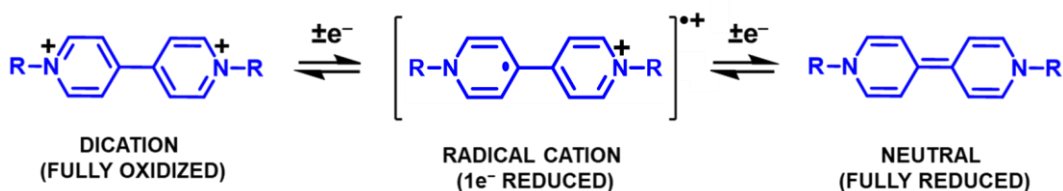


Figure 2.1 The three oxidation states of alkyl viologens

### 2.1.1 Viologen Dication

Viologens were first synthesized in 1882 by Weidel and Russo<sup>7</sup> using a method commonly still used today, namely the reaction of 4,4'-bipyridine with an alkyl halide, such as methyl iodide, under reflux. In the  $V^{2+}$  state they are incapable of aggregating together due to the repulsive coulombic forces that result from the positive charges on each viologen.

### 2.1.2 Viologen Radical-Cation

The redox properties of viologen salts were first investigated by Leonor Michaelis, of Michaelis-Menton kinetics fame, in the early 1930's.<sup>2</sup> Due to the combination of the color change between  $V^{2+}$  and  $V^{•+}$ , as well as the reduction potential between them being  $\sim -0.4$  V, Michaelis saw them as a potential redox indicator in biological systems, where they are still commonly used today.<sup>10,11</sup> The redox properties of viologens were further investigated by Kosower and Cotter<sup>12</sup> in the mid-1960's, where they determined that the variance in color of  $V^{•+}$  at different concentrations was due to dimerization (Fig 2.2). At low concentrations in water, most viologens will not dimerize, resulting in a bright blue color. At higher concentrations,  $V^{•+}$  dimerizes, leading to a violet-purple color.

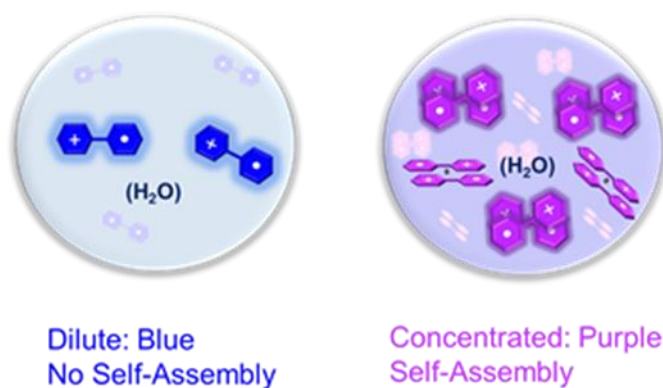


Figure 2.2 Left: Dilute methyl viologen in water is incapable of spin-pairing. Right: Concentrated methyl viologen in water is a violet-purple color due to spin-pairing dimerization.

Upon a one-electron reduction,  $V^{2+}$  is reduced to  $V^{•+}$ , the radical-cation. In this oxidation state, many of the more interesting properties of viologens are observed. The radical is somewhat stable due to the viologen's conjugated system, often taking minutes to oxidize back to  $V^{2+}$  in solution when exposed to oxygen.<sup>1</sup> This process is highly reversible, allowing it to be cycled many times without significant side reactions. Its reversible redox chemistry has allowed it to be used as the anolyte redox-flow batteries.<sup>8,9</sup> The radical-cation  $V^{•+}$  is also highly colored, a stark



contrast to the colorless  $V^{2+}$ .<sup>2</sup> In water,  $V^{*+}$  is a blueish-violet color, depending upon concentration. This color change is what led Leonor Michaelis to term them “viologens.”<sup>2</sup>

### **2.1.3 Neutral Viologen**

The radical cation  $V^{*+}$  can be further reduced to  $V^0$ , the neutral species. This species is the least utilized of the three oxidation states and is a yellowish-orange/brown color.<sup>2</sup> Part of the reason for its lack of experimental use is its reactivity.<sup>13</sup> It is roughly 1000 times more reactive to both acids and oxygen, making it incredibly unstable and difficult to work without it being oxidized to either charged state. The neutral  $V^0$  is also much more nonpolar than either the  $V^{2+}$  or  $V^{*+}$ , causing it to often precipitate from solutions that are soluble to the two charged species. Both the rapid oxidation and solubility cause  $V^0$  to be utilized less than  $V^{*+}$  in most circumstances, though it has been investigated for potential applications such as an n-type dopant for carbon nanotubes.<sup>14</sup>

## **2.2 Intramolecular Viologens**

### **2.2.1 Viologen Tethers**

One method that has been widely used to remove the concentration-dependent aspect of viologen radical cation dimerization is the incorporation of multiple viologen moieties into a single molecule.<sup>15</sup> This can be most simply accomplished by linking two viologen units via an alkyl tether, such as by reacting 1,3-dibromo propane with excess mono-methyl viologen, though it can also be accomplished by incorporating viologens into a polymer. Viologen polymers have two main variants: one with the viologens incorporated into the main chain of the polymer, and the second by having the viologen as a pendant group “dangling” off of the side.

### 2.2.2 Effect of Viologen Tethers on Dimerization

The length and type of tether used to separate viologens has a large impact on the ability of viologens to dimerize.<sup>15</sup> Of the simple alkyl tethers, the dimerization of the viologens is strongest with a propyl three carbon spacer. This has the optimal bond angles to allow the viologens to be in as close of proximity to each other as possible. The stability and intensity of this interaction weakens as the alkyl tether becomes longer, preventing the viologens from being close together. This can be most easily seen using UV-Vis-NIR (Fig. 2.3). A band in the 500-600 nm range is indicative of viologen radical-cations, while presence of a band in the ~850 nm area indicates the radical self-recognition, with the stronger band indicating the strength of the interaction.

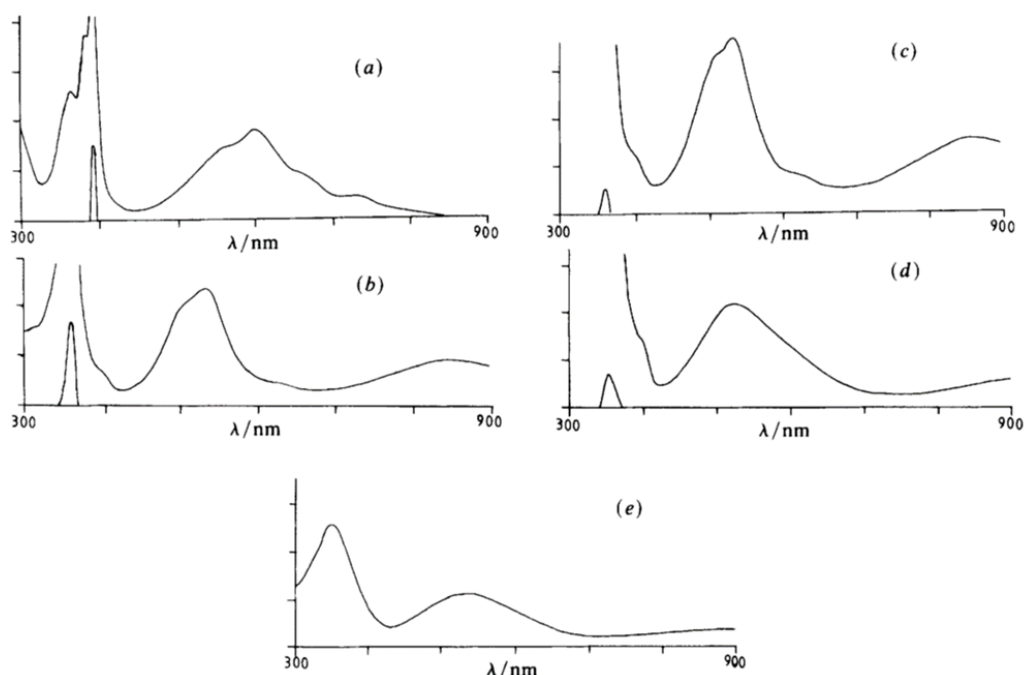


Figure 2.3 UV-Vis-NIR traces done of viologens reduced with sodium dithionite in water. a) Methyl viologen, no interaction; b) dimer viologen with 3-carbon tether; c) *ortho*-viologen dimer; d) *meta*-viologen dimer; and e) *para*-viologen dimer. Adapted from ref. [15].

Viologens can also be separated by benzene spacers, most commonly done by reacting a viologen precursor such as mono-methyl viologen with dibromo-xylene.<sup>15,16</sup> Just as with alkyl tether length, the position of the substituents has a large effect on the ability of viologens radical-

cations to dimerize. The *ortho*-substituted benzene viologens, when dimerized upon reduction to the radical-cation, are incredibly stable due to the close proximity, with a similar reduction potential to the propyl-viologens. *Meta*-substituted benzene viologens are capable of dimerizing, though the interaction is much weaker and more reversible. *Para*-viologens are entirely incapable of dimerization, the linear linker preventing any intramolecular stacking.

This *p*-xylene linker is useful in scenarios in which the redox-active properties of viologens are required in a single molecule without intra-molecular stacking, perhaps best utilized by Stoddart and co-workers in the creation of cyclobis(paraquat-*p*-phenylene), **CBPQT**<sup>4+</sup> or “blue-box,” and its derivatives (Fig 2.4).<sup>16</sup> By creating a cyclic molecule composed of two viologens separated by *p*-xylene spacers, **CBPQT**<sup>4+</sup>, this allows for molecular self-recognition between the host viologens of the reduced **CBPQT**<sup>2(•+)</sup> and a guest viologen, with the cavity between the viologens of **CBPQT**<sup>2(•+)</sup> being the perfect size for a small monomeric viologen, such as methyl viologen, forming the **MV**<sup>•+</sup>⊂**CBPQT**<sup>2(•+)</sup> tris-radical inclusion complex. Since this interaction relies upon the viologen radical self-recognition, it allows for this complex to be disrupted upon oxidation, with the columbic repulsion between cations, forcing the guest viologen out.

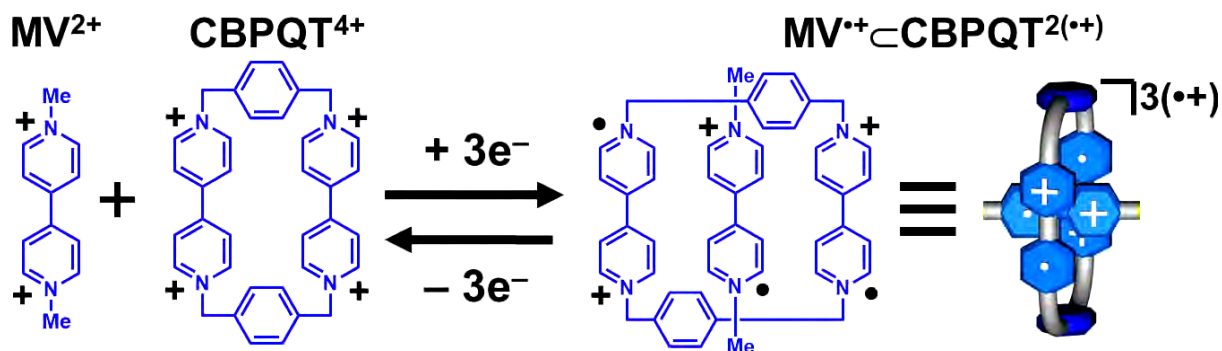


Figure 2.4 Schematic (left) and visual (far right) representations of the tris-radical inclusion complex of **MV**<sup>•+</sup>⊂**CBPQT**<sup>2(•+)</sup> due to spin-pairing effects. Adapted with permission from ref. [16].

## 2.3 Viologen Applications in Hydrogel Actuators

Until the J. Barnes group began its preliminary work in 2016,<sup>17</sup> no one had explored the use of viologen radical-cation self-recognition to actuate soft materials, though there has been emerging interest since that initial publication.<sup>21</sup> Viologens have been incorporated into hydrogels for a number of other applications, however, such as redox-responsive sol/gel transitions using host-guest chemistry with pillar[5]arene<sup>18</sup> or cucurbit[8]uril (CB[8]),<sup>19</sup> or used as a redox mediator for hydrogenase proteins bound to a polymer network.<sup>20</sup>

### 2.3.1 Introduction

In that initial publication, we reported the synthesis and application of a series of highly water-soluble, unimolecular main-chain oligoviologens as a potential cheap, robust, and redox-responsive means of reversibly actuating cubic-centimeter-sized hydrogels. This novel redox-based mechanism of actuation involves the reduction of  $V^{2+}$  to  $V^{•+}$ . This reduction results in the decrease of electrostatic repulsion and loss of the corresponding counteranion, followed by the intramolecular collapse of the viologen-containing oligomer as the viologens undergo noncovalent radical-based self-assembly. This mechanism can be likened to the collapse of an accordion, where this chain collapse as a result of viologen self-assembly leads to a decrease in chain length and mass, ultimately reducing the mesh size of the three-dimensional hydrogel network. This combination of the loss of counteranions and electrostatic repulsion and reduction in mesh size causes the loss of water from the system and contraction of the bulk hydrogel.

### 2.3.2 Oligoviologen Synthesis

The viologens oligomers were synthesized (Fig 2.5) using an iterative synthesis with alternating substitution reactions to grow the oligomer in a sequence-defined manner. Briefly the  $2V^{2+}$  was reacted with 20 equivalents of ditosylated hexaethylene glycol (**HEG-Tos**) at 130°C / high pressure (HP) to yield  $2V^{4+}$ . This  $2V^{4+}$  with terminal tosylates was reacted with 20 equivalents of

4,4'-bipyridine, also at 130 °C / HP, to yield  $4V^{6+}$ . These two reaction steps can then be repeated to grow the oligomers, with an additional viologen added every time the cycle is repeated. At any chain length that terminates in a pseudo-viologen, i.e.  $nV^{(2n+2)}$ , the chain growth was halted by the reaction of the bipyridine-capped chain with Tos-DEG-N<sub>3</sub> at 130°C / HP to yield the azide-capped  $nV^{(2n)}-N_3$ .

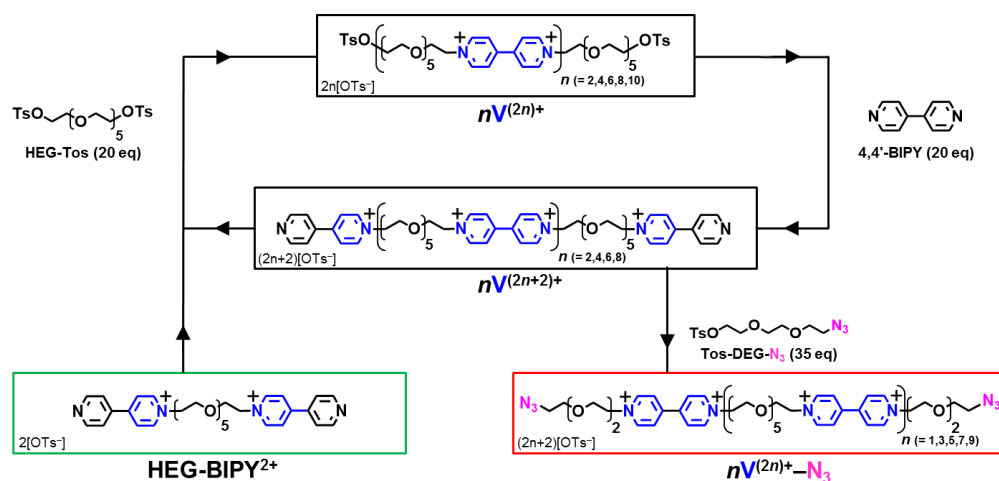


Figure 2.5 Schematic of the iterative synthesis of sequence-defined oligoviologens.

The ability of these oligoviologens to undergo pimerization-induced intramolecular chain collapse was confirmed by UV-vis-NIR in MeCN and water where each oligomer was reduced to the corresponding radical cation by addition of Zn<sup>0</sup> or 1 M sodium dithionite (Na<sub>2</sub>S<sub>2</sub>O<sub>4</sub>) respectively. The broad band at ~870 nm is indicative of viologen pimerization. This band undergoes a bathochromic (red) shift as the number of viologens per oligomer increases, indicating an increase in viologen radical-cation stacking to include tris-radical complexes of three viologens (Fig 2.6).

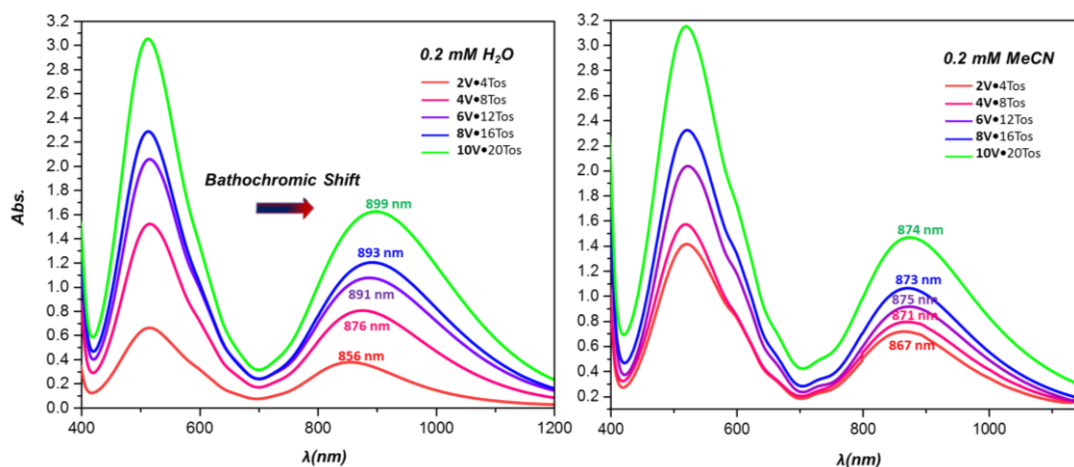


Figure 2.6 UV-Vis-NIR traces of oligoviologens of different lengths in (left) H<sub>2</sub>O and (right) MeCN.

### 2.3.3 Viologen-Containing Hydrogel Preparation

To test the color change and rate of actuation of viologen-containing hydrogels, such hydrogels were made using 5 mol % azide end-capped  $nV^{(2n)+}$ , 95 mol % azide end-capped polyethylene glycol (PEG-N<sub>3</sub>,  $M_n = 2000$ ), and 0.5 equivalent of a tetra-alkyne crosslinker (TAXL) via azide-alkyne cycloaddition “click” reaction (Table 2.1). These hydrogels were capable of being made in many types of molds, such as the preparation of disks using rubber septa or vial caps, cubes using silicon candy molds, to even more complicated shapes, such as flowers or bears. After preparation, the gels were immersed in 0.2 M ethylenediaminetetraacetic acid (EDTA) ligand in phosphate buffered saline (PBS) for 24 hours to remove any residual copper metal used in the gelation procedure.

Oligoviologen (OV)	Moles of OV (oligoviologen gel)	Total Moles of Viologen	Moles of 1V•2Tos-N <sub>3</sub> (Monoviologen gel)
2V <sup>4+</sup>	$2.3 \times 10^{-6}$	$4.6 \times 10^{-6}$	$4.6 \times 10^{-6}$
4V <sup>8+</sup>	$2.3 \times 10^{-6}$	$9.2 \times 10^{-6}$	$9.2 \times 10^{-6}$
6V <sup>12+</sup>	$2.3 \times 10^{-6}$	$1.38 \times 10^{-5}$	$1.38 \times 10^{-5}$
8V <sup>16+</sup>	$2.3 \times 10^{-6}$	$1.8 \times 10^{-5}$	$1.8 \times 10^{-5}$
10V <sup>20+</sup>	$2.3 \times 10^{-6}$	$2.3 \times 10^{-5}$	$2.3 \times 10^{-5}$

Table 2.1 Table indicating the moles of viologen per gel. (Left) is the number of mols of oligoviologen chain need to achieve a given total moles of viologen. (Right) Moles of mono-viologen needed to match the number of viologens in each oligomer incorporated into a hydrogel

### 2.3.4 Kinetics of Actuation

To determine how the length, and thus molecular weight, of the oligoviologen chains affected the contraction rate and amount, kinetic studies were carried out. Each hydrogel would only differ in the length of oligoviologen, with identical mol %, and thus crosslinking density, maintaining the same crosslinking density in each hydrogel.

To measure the rate of contraction, each viologen-containing hydrogel was submerged in 1 M  $\text{Na}_2\text{S}_2\text{O}_4$  under nitrogen atmosphere. Though the reduction can be done in the presence of oxygen, the  $\text{Na}_2\text{S}_2\text{O}_4$  is required to compete with the oxidation process, slowing the reduction. The submergence of the hydrogels in a  $\text{Na}_2\text{S}_2\text{O}_4$  solution results in a rapid change in color from colorless to deep purple (Fig. 2.7), with the gel becoming darker, almost black, as the reduction continues. The reduction was conducted over the course of several hours in order to get the fully reduced size. The final contracted volume was measured by the percent ratio (final/initial) between the starting volume of the fully swollen hydrogel and final reduced volume. Also, a viologen-containing chain with only one viologen moiety ( $\text{1V}^{2+}$ ) that is incapable of chain folding was synthesized to determine the effect of chain folding on actuation.

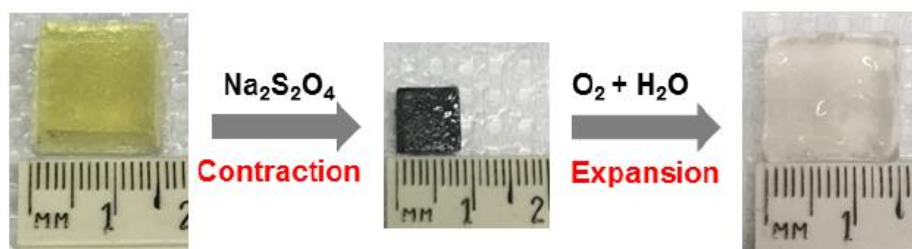


Figure 2.7 Images of a viologen cube losing size and changing color as it reduces, followed by expansion and reoxidation in water.

A clear trend is observed when examining the contraction data across all oligoviologen samples. Generally, both the rate and degree of contraction grows larger as more viologen subunits are introduced into the oligoviologen chains incorporated into the polymer network. A plateau is

reached at the  $10V^{20+}$  hydrogels, with maximum contraction down to 9% of their original volume(Fig 2.8). This may be attributed to the fact that the higher molecular weight oligoviologens lose a greater number of positive charges, thus a greater number of negative counteranions, after the introduction of the chemical reductant compared to the shorter length chains. Of note is that the intramolecular chain folding does play a significant impact on the rate and amount of contraction, as even when  $1V^{2+}$  with identical mols of viologen to a longer chain were made (Table 2.1, Fig. 2.8), they displayed less overall contraction compared to the extended chains. Similar kinetic behavior was also observed for both cube- and disc-like hydrogels, indicating a lack of shape dependency.

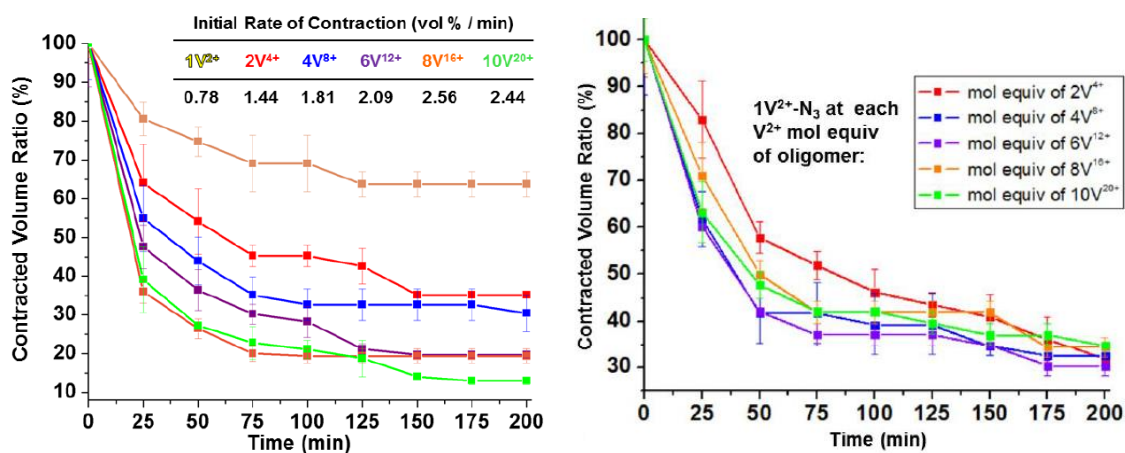


Figure 2.8 (Left) Rate of actuation of each hydrogel with 5 mol % oligoviologen incorporated and (Right) rate of actuation of mono-viologen-containing hydrogels with equivalent moles of viologen for each chain.

The cause of the change in size and mass is attributed to a number of factors, such as the collapse of the oligoviologen chains due to viologen pimerization, the loss of counterions as negative ions leave the network and take water with them, but this drastic loss in size and mass can mainly be attributed to the decrease in electrostatic repulsion. These viologen-containing hydrogels were cycled a number of times to ensure that reactivity was not lost upon oxidation and reduction



cycles. Of note is that only the oxidized hydrogel is capable of swelling, requiring both oxygen and water to regain its swollen state.

### 2.3.5 Mechanical Properties

We also sought to ascertain the effect that reduction had on the mechanical properties of the hydrogel material as the contracted state possessed decreased mesh size and contained less water. To characterize the mechanical behavior of the contracted and expanded hydrogel states, oscillatory shear rheology was used on disc-shaped  $6V^{12+}$ -containing hydrogels. A frequency sweep (at 1% strain amplitude) from 0.1 to 100 rad/s was done on both the reduced and oxidized hydrogels in order to identify whether or not any viscous behavior could be observed at higher frequencies (Fig. 2.9). For both states, at no point did it exhibit a crossover point (when  $G'$  falls below  $G''$ ) even at high frequencies, indicating that the behavior of the hydrogels is elastic at all frequencies. What was observed was a  $\sim 2.5$  fold increase in the  $G'$  for the contracted state in comparison to that of the swollen state, indicating that the contracted state is much stiffer than when it is swollen.

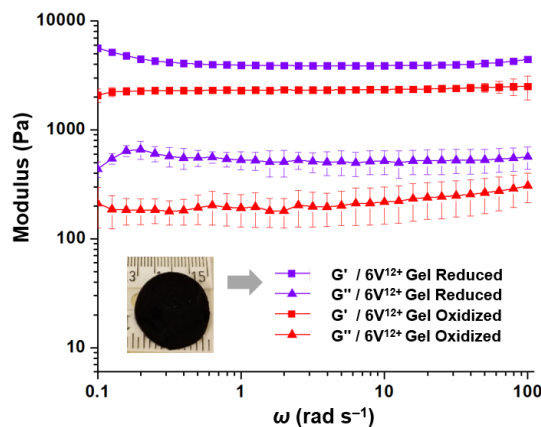


Figure 2.9 Comparison of the characteristics of a  $6V^{12+}$  hydrogel between the contracted and swollen state using a frequency sweep at 1% strain amplitude.

### 2.3.6 Scalability

As an example of the scalability of our actuating hydrogel, we created a cubic  $6V^{12+}$ -containing hydrogel and placed it into  $N_2$ -sparged glass jar. A dime was placed on top of the hydrogel and it was allowed to contract in a 1 M  $Na_2S_2O_4$  solution. The height of the dime was monitored over several hours as the gel contracted, and after no further change occurred, the gel was allowed to oxidize back, lifting the dime (Fig. 2.10). This demonstrated the ability of the hydrogel to work, with a 2.028 g dime lifted 3.0 mm by a 377 mg hydrogel that is ~95% water.

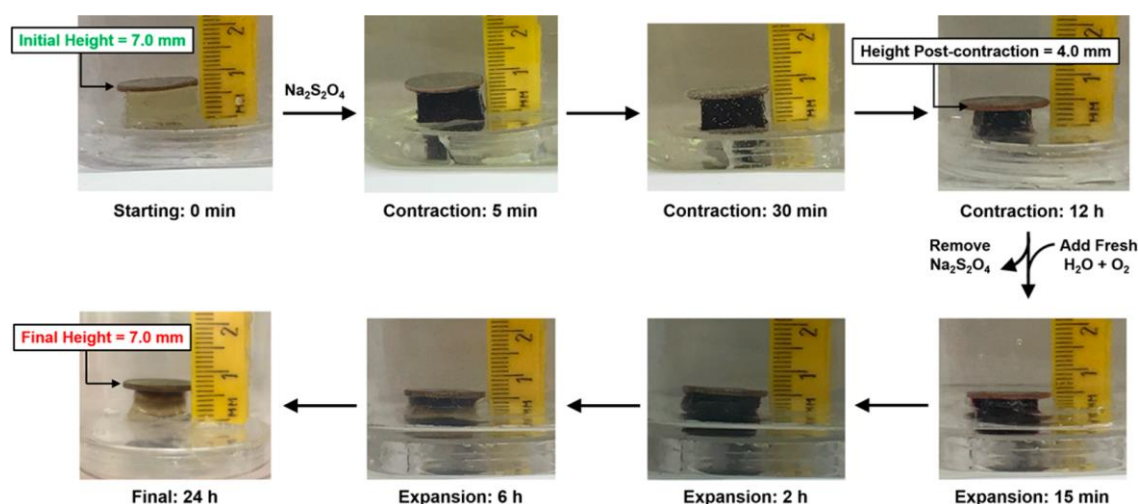


Figure 2.10 Images of the  $6V^{12+}$  cube performing work by lowering then lifting a dime.

### 2.3.7 Conclusion

With this initial publication, the ability of redox-responsive oligoviologens to actuate bulk-scale materials reversibly was demonstrated. The viologen content of the longer chains was shown to actuate the material both faster and to a greater degree, with this effect plateauing at  $8V^{16+}$ . The mechanical properties were shown to change between the swollen and contracted states, with the contracted material displaying a 2.5-fold increase in  $G'$  over its swollen counterpart. The foundation was laid for a new and more flexible method of actuation. One of the strongest aspects of the viologen actuation platform is the variety of methods by which a redox mechanism

can be facilitated, each of which could be a novel mechanism by which viologen-containing hydrogels could be actuated.

## References: Chapter 2

1. Bird, C. L., Kuhn, A. T. Electrochemistry of the viologens. *Chem. Soc. Rev.* **1981**, *10*, 49–82
2. Michaelis, L., Hill, E. S. The Viologen Indicators. *J. Gen. Physiol.* **1933**, *16*, 859–873
3. Li, H., Zhu, Z., Fahrenbach, A. C., Savoie, B. M., Ke, C., Barnes, J. C., Lei, J., Zhao, Y.-L., Lilley, L. M., Marks, T. J., Ratner, M. A., Stoddart, J. F. Mechanical Bond-Induced Radical Stabilization. *J. Am. Chem. Soc.* **2013**, *135*, 456–467
4. Barnes, J. C. et al. A Radically configurable six-State Compound. *Science* **2013**, *339*, 429–433
5. Ito, T., Ujiie, T., Naka, M., Nakamura, H. Photoinduced electron transfer and its magnetic field dependence in supramolecular complex of zinc(II) tetraphenylporphyrin-viologen chain-linked compound with 2,3,6-tri-*O*-methyl- $\beta$ -cyclodextrin. *Chem. Phys. Lett.* **2001**, *340*, 308–316
6. Tiah, F., Jiao, D., Biedermann, F., Sherman, O. A. Orthogonal switching of a single supramolecular complex. *Nat. Commun.* **2012**, *3*, Article number: 1207.
7. Weidel, H., Russo, M. *Monatsh. Chem.* **1882**, *3*, 850–885.
8. Nagarjuna, G. et al. Impact of Redox-Active Polymer Molecular Weight on the Electrochemical Properties and Transport Across Porous Separators in Nonaqueous Solvents. *J. Am. Chem. Soc.* **2014**, *136*, 16309–16316.
9. Janoschka, T., Martin, N., Martin, U., Friebe, C., Morgenstern, S., Hiller, H., Hager, M. D., Schubert, U. S. An aqueous, polymer-based redox-flow battery using non-corrosive, safe, and low-cost materials. *Nature* **2015**, *527*, 78–81
10. Fultz, M. L., Durst, R. A. Mediator compounds for the electrochemical study of biological redox systems: a compilation. *Anal. Chim. Acta* **1982**, *140*, 1–18.
11. Sen, S. et al. Molecular characterization of two novel proteins All1122 and Alr0750 of *Anabaena* PCC 7120 conferring tolerance to multiple abiotic stresses in *Escherichia coli* *Gene*, **2018**, <https://doi.org/10.1016/j.gene.2018.11.038>
12. Kosower, E. M., Cotter, J. L. Stable Free Radicals. II. The Reduction of 1-Methyl-4-cyanopyridinium Ion to Methylviologen Cation Radical *J. Am. Chem. Soc.* **1964**, *86* (24), 5524–5527.
13. Mohammad, M. Methyl Viologen Neutral MV<sup>•+</sup>: 1. Preparation and Some Properties *J. Org. Chem.*, **1987**, *52* (13), 2779–2782.
14. Kim, S. M. et al. Reduction-Controlled Viologen in Bisovent as an Environmentally Stable n-Type Dopant for Carbon Nanotubes. *J. Am. Chem. Soc.* **2009**, *131*, 327–331.
15. Neta, P., Richoux, M-C. Intramolecular Association of Covalently Linked Viologen Radicals *J. Chem. Soc., Faraday Trans. 2*, **1985**, *81*, 1427–1443.
16. Fahrenbach, A. C., Barnes, J. C. et al. Solution-Phase Mechanistic Study and Solid-State Structure of a Tris(bipyridinium radical cation) Inclusion Complex. *J. Am. Chem. Soc.* **2012**, *134*, 3061–3072.

17. Greene, A. F.; Danielson, M. K.; Delawder, A. O.; Liles, K. P.; Li, X.; Natraj, A.; Wellen, A.; Barnes, J. C.: Redox-Responsive Artificial Molecular Muscles: Reversible Radical-Based Self-Assembly for Actuating Hydrogels. *Chem Mater.*, **2017**, *29* (21), 9498–9508.
18. Li, H. et al. Viologen-Mediated Assembly of and Sensing with Carboxylatopillar[5]arene-Modified Gold Nanoparticles. *J. Am. Chem. Soc.*, **2013**, *135*, 1570–1576.
19. McKee, J. R. et al. Healable, Stable and Stiff Hydrogels: Combining conflicting Properties Using Dynamic and Selective Three-Component Recognition iwht Reinforcing Cellulose Nanorods. *Adv. Funct. Mater.* **2014**, *24*, 2706–2713.
20. Plumere, N. et al. A redox hydrogel protects hydrogenase from high-potential deactivation and oxygen damage. *Nat. Chem.* **2014**, *6*, 822–827.
21. Wang, B., Tahara, H., Sagara, T. Driving Quick and Large Amplitude Contraction of Viologen-Incorporated Poly-L-Lysine-Based Hydrogel by Reduction. *ACS Appl. Mater. Interfaces*, **2018**, *10*, 36415–36424.

# **Chapter 3: A Photoredox Responsive Hydrogel Actuator**

This chapter is based on research described in the following work: Liles K. P.; Greene, A. F.; Danielson, M. K.; Colley, N. D.; Wellen, A.; Fisher, J. M.; and Barnes, J. C.: Photoredox-Based Actuation of an Artificial Molecular Muscle. *Macromol. Rapid Commun.* **2018**, *39*, 1700781

The use of light to actuate materials is advantageous due to it representing a cost-effective and operationally simple method to introduce energy into a stimuli-responsive system. Here, a novel mode of actuation in a series of redox-responsive hydrogels were doped with a visible-light-absorbing ruthenium-based photocatalyst. These redox-responsive hydrogels were composed primarily of poly(ethylene glycol) (PEG) with low molar concentrations of our redox-responsive oligoviologen. The rate and degree of actuation was found to be ~50% after five hours of irradiation with blue light. Likewise, the mechanical properties were assessed as a function of oligoviologen concentration, with the 5 mol% being the optimum concentration of oligoviologen for both stiff mechanical properties and rapid actuation. Last, an artificial molecular muscle was fabricated using this optimal hydrogel composition and shown to perform work while irradiated.

## **3.1 Introduction**

One of the challenges in stimuli-responsive materials involves the design of macromolecular systems by converting external stimuli into useful macroscopic work. Of the many types of stimuli that can be used, such as temperature,<sup>1</sup> changes in pH,<sup>2,3</sup> etc., the use of light as that stimuli source is attractive since its versatility allows for spatial and temporal control over the actuation process. The most common approach to program light responsiveness involves the incorporation of azobenzene-containing polymers<sup>4,5</sup> because the synthesis to prepare them is

relatively straightforward and the UV *trans-to-cis* photoisomerization is well characterized. Similarly, spiropyrans<sup>6,7</sup> have been investigated in light-responsive hydrogels actuators, as well as others that employ gold<sup>8</sup> or graphene oxide nanoparticles.<sup>9</sup>

We had previously reported a redox-responsive hydrogel system<sup>10</sup> that was prepared via copper-mediated “click” chemistry and composed of PEG 5 mol% of redox-active, unimolecular oligoviologens, and a tetra-alkyne crosslinker. Although sodium dithionite ( $\text{Na}_2\text{S}_2\text{O}_4$ ) is an effective method for actuating large hydrogels quickly, it does not allow for spatial or temporal control over actuation kinetics (Fig 3.1).

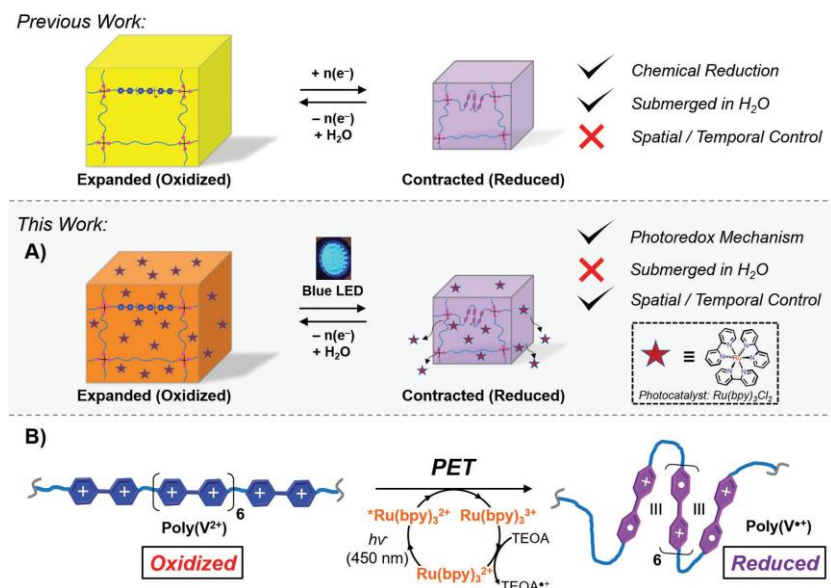


Figure 3.1 (Top) The visual representation of the previous, chemically induced, hydrogel contraction. (Middle) Concept for light-induced contraction and expansion of a hydrogel along with the PET cycle utilized (bottom).

## 3.2 Photoelectron Transfer

With the success of using  $\text{Na}_2\text{S}_2\text{O}_4$  as a chemical reductant for our viologen actuator, we sought to achieve photoinduced electron transfer (PET) from tris (2,2'-bipyridine) ruthenium (II) chloride  $[\text{Ru}(\text{bpy})_3]^{2+*}$  to each viologen subunit in the  $\mathbf{8V}^{16+}$  oligomer chain, the length of viologen oligomer that showed the best rate of actuation in our previous study (Figure 3.1

bottom).  $[\text{Ru}(\text{bpy})_3]^{2+}$  is a well-known photosensitizer<sup>11</sup> that is capable of reducing viologen moieties via PET when exposed to 450 nm blue light.<sup>12</sup> This approach expands the versatility of the viologen actuatable platform, as it allows actuation without submersion in a redox solution, and also allows for temporal control.

To ensure that  $[\text{Ru}(\text{bpy})_3]^{2+}$  is still capable of reducing oligomeric viologens, UV-Vis-NIR studies were carried out (Fig. 3.2). The oligomeric viologen by itself or with the  $[\text{Ru}(\text{bpy})_3]^{2+}$  and sacrificial electron donor triethanolamine (TEOA) in the dark showed no absorption bands in the 515 or ~875 nm range, indicative of a lack of viologen reduction and pimerization. After irradiation for an hour in the presence of both  $[\text{Ru}(\text{bpy})_3]^{2+}$  and TEOA, hereafter called “photoredox” solution, both bands are present in the trace, confirming the ability of  $[\text{Ru}(\text{bpy})_3]^{2+}$  to reduce the oligomeric viologens upon excitation and allow them to undergo radical molecular self-recognition.

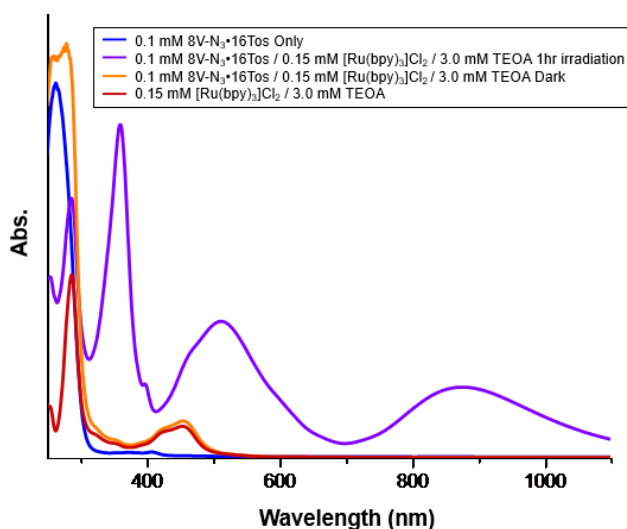


Figure 3.2 UV-Vis-NIR trace of  $8\text{V}^{16+}$  (blue), “photoredox” solution (red), both mixed without (yellow) and with (purple) exposure to a light source.

### 3.3 Photo-responsive Hydrogel Characterization

PEG-N<sub>3</sub> ( $M_n = 2000 \text{ g mol}^{-1}$ ), **8V<sup>16+</sup>-N<sub>3</sub>**, and the tetra-alkyne crosslinker were synthesized and incorporated into a three-dimensional hydrogel network using our previously shown method. In these hydrogels, the molar ratios between PEG and **8V<sup>16+</sup>-N<sub>3</sub>** were chosen to incrementally increase the redox-responsive component incorporated into the hydrogels to determine if higher molar amounts of oligoviologen (i.e. 0, 1, 5, 10, and 20 mol%) would result in greater rates and degrees of actuation. Once the gels had been synthesized, they were swollen in N<sub>2</sub>-sparged aqueous solution containing  $0.15 \times 10^{-3} \text{ M}$  [Ru(bpy)<sub>3</sub>]Cl<sub>2</sub> and  $3.0 \times 10^{-3} \text{ M}$  TEOA for 24 hours, the “photoredox” solution, in an N<sub>2</sub>-filled glovebox.



Fig. 3.3 Experimental setup for blue-light irradiation.

For actuation, each of the desired gels were removed from the “photoredox” solution and placed into a sealable glass jar (Fig. 3.3). Each jar also contained a damp Kimwipe to maintain the humidity inside the jar and mitigate any dehydration due to the arid conditions of the glovebox. The jar containing both the desired gels and the Kimwipe was then clamped in between two lamps equipped with blue light-emitting diode (LED) bulbs. The hydrogels were then irradiated and the volume of each hydrogel was measured at 0, 30, 60, 120, 180, and 300 min by removing them from the jar and measuring with a caliper. As would be expected, the hydrogels went from



a yellow-orange color to a deep purple, almost black, color as irradiation progressed and radical-cation pimerization of the viologen chains occurred.

### 3.3.1 Kinetics of Photo-Responsive Viologen Hydrogels

As stated previously, the volume of each hydrogel was measured at 0, 30, 60, 120, 180, and 300 min in order to ascertain the rate of actuation between different mol % of redox-active viologen chains. As shown in Figure 3.4, the gel with no viologens lost roughly 10% of its total volume over five hours, likely due to dehydration. This dehydration could potentially be attributed to low levels of heat caused by the blue light as well as the brief expose of the hydrogels to the arid glovebox environment each time it was measured.

The 5, 10, and 20 mol% oligoviologen-containing hydrogels all contracted at the same rate and ended at the same volume (Fig. 3.4), with no statistical difference in their datasets, ending at approximately 50% of their final volume. The 1 mol% actuation trace is between the 0 mol % control and the three higher concentrations, ending at about 80% of its final volume. This indicates that the rate and amount of contraction plateaus at 5 mol %, with increases to 10 and 20 mol% giving no appreciable performance change.

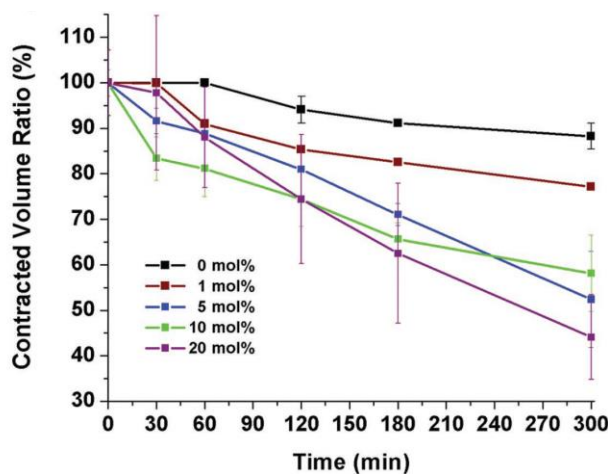


Figure 3.4 Kinetic data for each mol % of  $8V^{16+}$  hydrogel

### 3.3.2 Mechanical Properties of Photo-Responsive Viologen Hydrogels

To quantify the differences in mechanical properties between each of the polyviologen-containing hydrogels, oscillatory shear rheology experiments were carried out on both contracted and expanded hydrogels. These hydrogels were obtained by “punching” out disc-shaped gels 20 mm in diameter from gels that were in either the contracted or swollen state. Each rheological experiment consisted of a frequency sweep from 0.1 to 100 rad s<sup>-1</sup> while keeping the strain constant at 1%. Interestingly, the data revealed that in the contracted state the storage moduli ( $G'$ ), i.e. the stiffness of the material, was the greatest in the 5 mol % hydrogel, followed by the 1 mol %, with the 10 and 20 mol % being the softest of the four materials (Fig. 3.5A). This indicates that although greater mol % of the  $8V^{16+}$  viologen chain causes an increase in the volume loss and stiffness of the material, incorporation of the 10 or 20 mol % causes weakening of the material. Thus, 5 mol % is the “sweet spot” in that it is the stiffest of the mol %’s attempted, as well as being the point at which the actuation kinetics begin to plateau, making the 5 mol % the best performing gel composition.

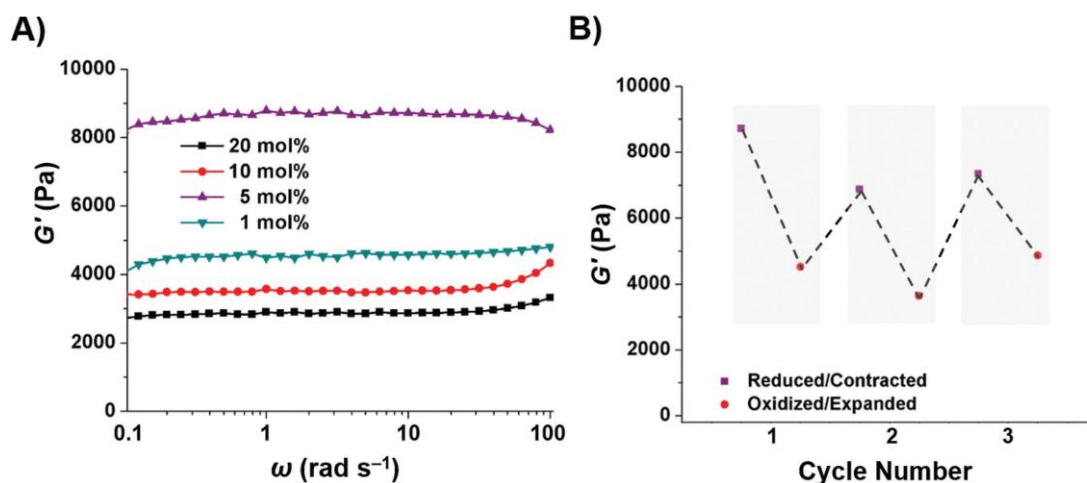


Figure 3.5 A) a table comparing the  $G'$  of each contracted hydrogel after irradiation for five hours. B) a graph of the  $G'$  value as a hydrogel is cycled through three contraction/expansion cycles.

To ensure that the material did not degrade over time, a set of gels were cycled between contracted/reduced and expanded/oxidized up to three times. At each point in this contraction/expansion cycle, oscillatory rheology was taken to ascertain the mechanical properties. As expected, the  $G'$  of the material in the oxidized/expanded state is roughly half that of the reduced/contracted state. Although some variability in  $G'$  is seen between cycles (Fig. 3.5B), the magnitude of each value remains consistent across cycles, demonstrating that the material can be cycled numerous times without noticeable degradation in mechanical properties.

### **3.4 Actuation of a Viologen Artificial Molecular Muscle**

In order to demonstrate our redox-responsive hydrogel's ability to do work, an artificial molecular muscle (AMM) was fabricated by taking a 3.1 x 0.4 x 3.1 cm rectangular strip of our best performing 5 mol %  $8V^{16+}$  hydrogel (503.0 mg swollen) to a piece of black electrical tape via commercial superglue. Excess tape outside the area of the hydrogel was cut away, leaving 2 cm of tape exposed on each end. The AMM was then moved inside the glovebox and submerged for 24 hrs in the "photoredox" solution containing the ruthenium-based photocatalyst and sacrificial reductant. The AMM had one side then clamped to the top of a glass jar using an epoxy resin, with the other end tethered via aluminum wire to a small sponge with a weight of 20.0 mg.

At  $t = 0$ , the AMM is almost linear as it hangs inside the jar. Blue light was then shined from one side, causing the PET process to reduce the viologen moieties and a color change from yellowish-orange to purple. The AMM bends as exposure time to the blue light is increased, ending with the AMM bent at nearly a  $90^\circ$  angle and the weight moved  $\sim 1.25$  cm right and 1.91 cm up (Fig. 3.6). This bending motion is because as the hydrogel contracts, it becomes shorter, forcing the tape to bend to continue to adhere to the shrinking hydrogel. That the weight of the

dried polymer in the hydrogel was only 19.0 mg demonstrated that the as-fabricated AMM is capable of lifting a mass roughly equal to its polymer weight, (20 mg). Of note is that ~5 mg of that weight is the redox-active viologen.

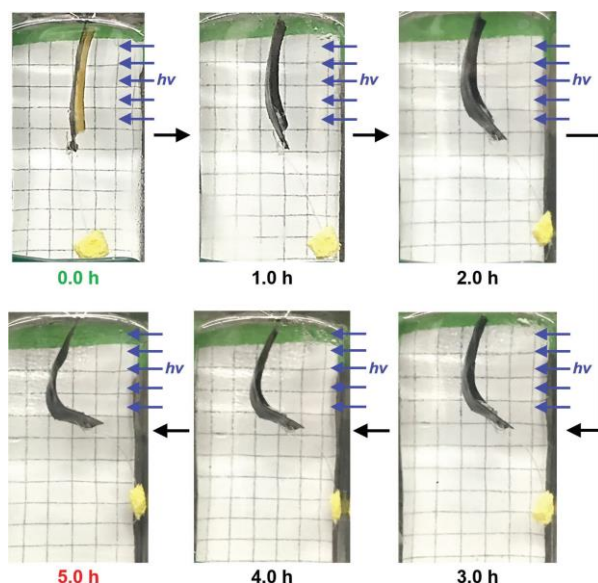


Figure 3.6 Images of the AMM as it undergoes work in response to a 450 nm light.

These results were compared with both a 5 mol %  $8V^{16+}$  hydrogel without a weight attached and a PEG-only 0 mol % viologen gel. The 5 mol % hydrogel was used to ensure that the results were reproducible, while the 0 mol % was to ensure that the motion observed in the AMM was not an effect of dehydration. As expected, the 5 mol %  $8V^{16+}$  hydrogel was observed to change black in color, with contraction causing the AMM to bend in the direction of the blue light. The PEG-only gel, which is not capable of photo-reduction, did not bend at all upon irradiation (Fig. 3.7), demonstrating the need for redox-active viologen oligomers to be present to cause the AMM to function and lift the weight.

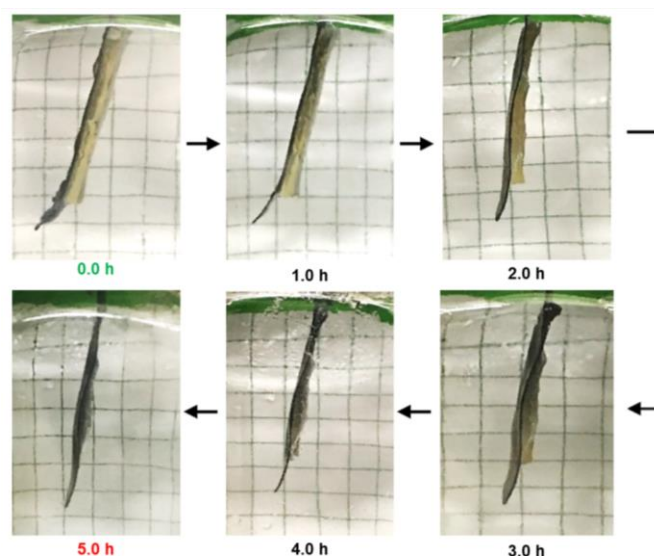


Figure 3.7 Images of a 0 mol % viologen, i.e. 100 mol % PEG, hydrogel as it is irradiated for five hours with blue light. It is not capable of actuating, thus only undergoes dehydration.

Though these results are highly encouraging, there are some limitations. For example, the AMM is slightly damaged after irradiation as a consequence of the poly(cyanoacrylate) superglue network that forms at the interface of the tape and the hydrogel. The light-activated contraction of the viologen hydrogel to be trapped in the superglue network as it shrinks, causing damage to the hydrogel. This limits the reversibility of the oligoviologen AMM when it is adhered to a different substrate. Nonetheless, this lays the foundation for future developments for more robust AMMs.

### 3.5 Conclusion

In this work, we describe a novel photoredox-based actuatable platform capable of doing work. This platform of unimolecular oligoviologen-containing hydrogels with only 1–20 mol % of the material being the redox-responsive component. Of these hydrogels, 5 mol % oligoviologen was determined to give the best combination of kinetics and stiffness, contracting down to ~50 % of its original volume after 5 hours and a  $G'$  of 8250 Pa. The hydrogel was also shown to maintain its mechanical properties over the course of several cycles. This optimal mol % hydrogel was

then used to perform work by lifting a weight of similar mass to that of the mass fraction of polymer inside the hydrogel. The inclusion of photo-irradiation as an energy source to actuate the material opens the door for potential applications such as drug delivery and wearable light-powered devices.

## 3.6 Experimental Information

### 3.6.1 Materials and Instrumentation

All reagents were purchased from commercial suppliers and used without further purification unless stated otherwise. Literature procedures were used in the synthesis of hexaethylene glycol di-*p*-toluenesulfonate (**HEG-Tos**),<sup>13</sup> 2-[2-(2-Azidoethoxy)ethoxy]ethyl-4-methylbenzene sulfonate (**Tos-DEG-N<sub>3</sub>**),<sup>14</sup> O,O'-Bis(2-azidoethyl)polyethylene glycol ( $M_n = 2000$ ) (**PEG-N<sub>3</sub>**),<sup>15</sup> tetrakis(2-propynyloxymethyl)methane (**TAXL**).<sup>16</sup> The protocol for the synthesis of **8V•14Tos** and the azide-capped polyviologen **8V-N<sub>3</sub>•16Tos**, was followed via the previously published procedure,<sup>10</sup> however an updated procedure demonstrating a large scale synthesis of **8V-N<sub>3</sub>•16Tos** is below. All photochemical reductions of polyviologen-containing hydrogels were performed under an inert atmosphere of UHP nitrogen to prevent premature reoxidation and were encapsulated in a humid environment to mitigate dehydration. Photochemical experiments were performed using two Hampton Bay desk lamps with ABI LED Aquarium Light Bulbs (12 Watt / 750 Lumens ea.) (Fig. 3.8). Ultraviolet-Visible-Near Infrared (UV-vis-NIR) absorbance spectra were recorded on an Agilent Cary 5000 spectrophotometer with a PbSmart NIR detector. Frequency sweep (1.0% strain, 0.1 to 100 rad s<sup>-1</sup>) and strain sweep (10 rad s<sup>-1</sup>, 0–200% strain) rheology experiments were carried out using a TA AR-G2 oscillatory shear rheometer with a 20 mm smooth geometry.

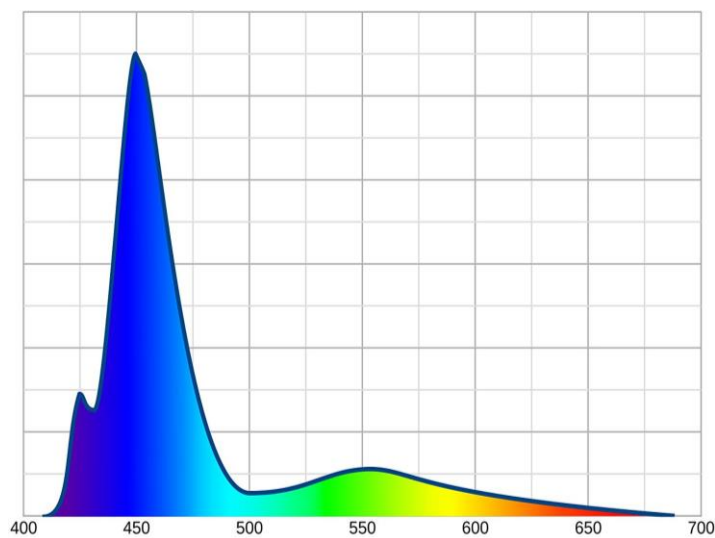


Figure 3.8 Emission spectrum of the ABI LED aquarium bulb used. Reprinted from ref [17].

### 3.6.2 Large-scale Synthesis of $8V-N_3 \cdot 16Tos$

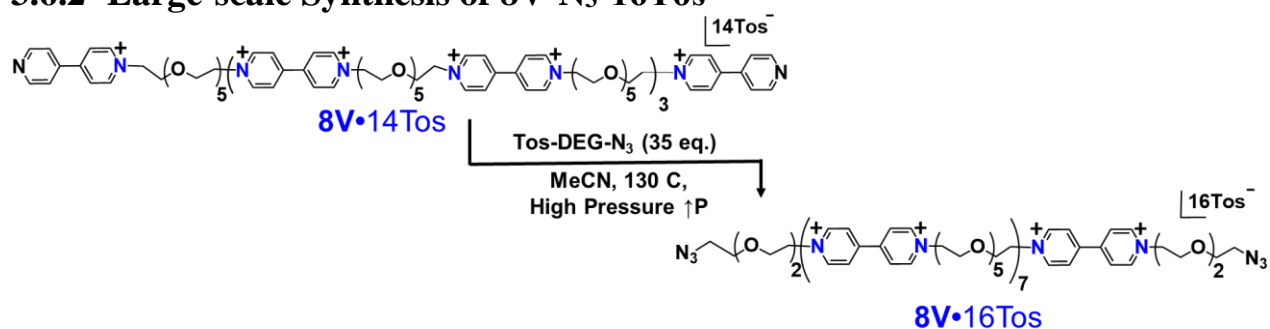


Figure 3.9 Scheme for the synthesis of  $8V^{16+} \cdot N_3$

Large scale Synthesis of  $8V-N_3 \cdot 16Tos$  (Fig. 3.9): A 100 mL thick walled high-pressure flask with Teflon screw cap and stir bar was charged with  $8V \cdot 14Tos$  (0.860 g, 0.170 mmol), **Tos-DEG-N<sub>3</sub>** (1.927 g, 5.57 mmol), and MeCN (30 mL). The flask was capped tightly, and the mixture was stirred at high-pressure at 130°C for 24 h. After 24 h, the reaction mixture was cooled to room temperature and the crude golden-brown mixture was transferred evenly to four 50 mL plastic centrifuge tubes and methanol (10 mL) was used to rinse any remaining material out of the reaction flask and evenly distributed among the four centrifuge tubes. PhMe (35 mL) was then added to the tubes to precipitate the pure product as a sticky brown oil. To assist in the

precipitation and purification of the product the MeCN/PhMe mixture was centrifuged twice at 4490 rpm at  $-10\text{ }^{\circ}\text{C}$  for 35 min, replacing the supernatant with fresh PhMe between runs. To maximize yields the MeCN/PhMe supernatant should be concentrated under reduced pressure and centrifuged a third time at identical conditions (1.48 g, 97 %).

### **3.6.3 General Procedure for Oligoviologen-containing Hydrogels**

**8V-N<sub>3</sub>•16Tos**, **PEG-N<sub>3</sub>**, and **TAXL** were weighed into a glass scintillation vial in appropriate ratios depending on the mole percent of the desired product and dissolved in DMF (0.6 mL). Then, CuSO<sub>4</sub> (7.2 mg, 0.046 mmol) and sodium ascorbate (4.6 mg, 0.046 mmol) were added to two separate 2-dram vials and each were dissolved in deionized water (0.2 mL). The CuSO<sub>4</sub> solution was then added via syringe to the solution of polymer/**TAXL** and vortexed for 5–10 seconds turning the solution a pale green color. The solution of sodium ascorbate was then slowly added to the pre-gel mixture and vortexed for another 5–10 seconds to ensure even distribution, a process which turned the solution a bright yellow. The gel mixture was then rapidly distributed by syringe into three separate 1 cm diameter Teflon molds. The gelation process was complete after approximately 30 min and the hydrogels were then transferred and swollen in an aqueous solution of ethylenediaminetetraacetic acid (**EDTA**) (0.05 M) overnight to remove excess copper ions remaining in the hydrogel. After swelling, the hydrogels were transferred to a fresh solution of DI water to wash the hydrogels and complete the swelling process.

### **3.6.4 Kinetic Procedure for Photo-redox Activation of Hydrogels**

Kinetics experiments were performed in triplicate, on gels containing 1, 5, 10, and 20 mol % polyviologen. The gels were fabricated, purified, and swollen in fresh H<sub>2</sub>O. The gels were then brought into an inert nitrogen glovebox environment and soaked for 24 h in a degassed aqueous



“photo-redox” solution containing  $[\text{Ru}(\text{bpy})_3]\text{Cl}_2$  (0.15 mM) and TEOA (3.0 mM) to serve as the photo-redox catalyst and sacrificial electron donor, respectively. The gels were then removed from solution and placed in a Kimble™ 8 oz. French Square bottle. A water-soaked tissue was also placed inside the bottle to provide ambient moisture. The lid of the bottle was covered in parafilm followed by electrical tape to prevent moisture escaping into the arid glovebox atmosphere. A PEG-only hydrogel was also soaked in the “photoredox” solution and similarly placed inside of a glass container containing a moist tissue to serve as a control. The two bottles, experimental and control, were suspended and irradiated with ~450 nm light from the top and bottom, maintaining a 5 cm distance between the gel and the light source at all times. The gels were irradiated for 12 h with diameter and height measurements taken at regular intervals. After irradiation, the gels were transferred to a fresh water solution in atmosphere to re-oxidize and swell.

### **3.6.5 Rheological Procedure for Photo-redox Activation of Hydrogels**

Gels were fabricated as stated previously. Gel solution was poured into a 2 cm diameter circular mold and allowed to set. The gels were then removed from the mold and submerged in EDTA solution [0.5 mM], and was replaced with fresh solution until it was colorless. Each gel was placed in a 3.5 cm petri dish and brought into the glove box, where it was soaked in “photoredox” solution for 12 h. A water-soaked tissue was then added to the petri dish, parafilm, and taped closed. The gels were then irradiated for 5 h from the top and bottom with ~450 nm light, removed from the light source, and a disc was punched out of the material 20 mm in diameter. The discs were placed into an airtight container, parafilm, and taped and rheological experiments were performed to obtain the reduced polyviologen-containing hydrogel data. The remaining gel material was removed from the nitrogen atmosphere and placed in water

to reoxidize and swell. The oxidized rheological data were then taken from a 20 mm disc gel sample that had been reduced once followed by reoxidation. 5 mol% gels were cycled to determine material strength over multiple contractions. A single cycle is defined by photochemical reduction under UHP nitrogen followed by re-oxidation in atmosphere, returning it to the fully oxidized state (Fig. 3.10).

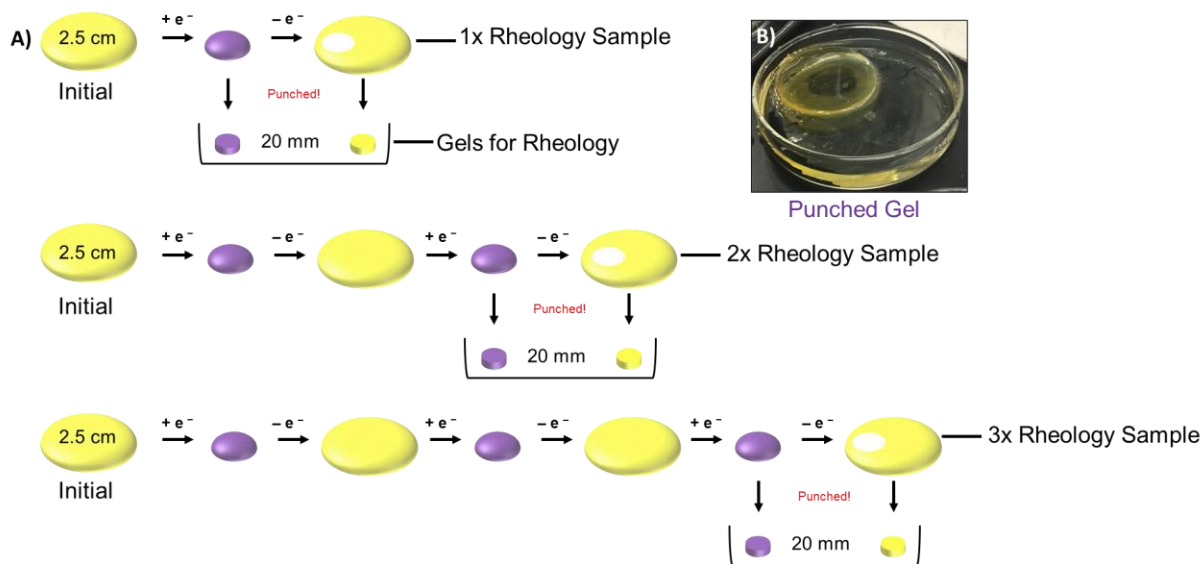


Figure 3.10 The rheological cycling of  $8v^{16+}$  hydrogels

### 3.6.6 Creation of Artificial Molecular Muscle

A strip of fully swollen polyviologen-containing gel was cut using a precision cutting tool to approximately 0.4 cm x 3.1 cm with an approximate mass of 500 mg. The excess moisture was gently dabbed away using a cotton tipped swab, while two 3.5 cm strips of black electrical tape were cut and pressed together with the adhesive sides turned inward to form one sturdy support. The black electrical tape support was then left under a flat heavy weight for 5 min to ensure that the support was straight and flat before gel adherence. Then, super glue was poured into a dish and a cotton tipped swab was thoroughly saturated in the glue and which was then applied to the portion of the tape where the gel was to be adhered. The glue was allowed to sit for 10 s to

become slightly tacky and the strip of polyviologen-containing gel was carefully placed on top of the glue using forceps and positioned so that it was as straight as possible, leaving 2 cm of tape exposed at the head and tail of the gel. Additional glue was then very quickly and carefully added to the outer edges of the gel to ensure that they were properly adhered. The adhesion of the gel to the tape was complete in approximately 1 min. Afterwards, the sides of the tape were cut to match the width of the hydrogel and the gel was then soaked in “photoredox” solution if the gel was to be activated photochemically, or in fresh water if the gel was to serve as a control experiment to monitor dehydration. The gels could not be reused after 5 h of experimentation due to damage (Fig. 3.11).



Figure 3.11 Dmaged AMM after 5 hours of irradiation.

## **References: Chapter 3**

1. Ron, E. S., Bromberg, L. E. Temperature-responsive gels and thermogelling polymer matrices for protein and peptide delivery. *Adv. Drug Delivery Rev.* **1998**, *31*, 197.
2. Dai, S., Ravi, P., Tam, K. C. pH-Responsive polymers: synthesis, properties, and applications. *Soft Matter* **2008**, *4*, 435.
3. Zhang, S. et al. A pH-responsive supramolecular polymer gel as an enteric elastomer for use in gastric devices. *Nat. Mater.* **2015**, *14*, 1065.
4. Nakahata, M., Takashima, Y., Hashidzume, A., Harada, A. Redox-Generated Mechanical Motion of a Supramolecular Polymeric Actuator Based on Host-Guest Interactions. *Angew. Chem. Int. Ed.* **2013**, *52*, 5731–5735.

5. Takashima, Y., Hatanaka, S., Otsubo, M., Nakahata, M., Kakuta, T., Hashidzume, A., Yamaguchi, H., Harada, A. Expansion-contraction of photoresponsive artificial muscle regulated by host-guest interactions. *Nat. Commun.* **2012**, 3:1270 doi: 10.1038/ncomms2280
6. ter Schiphorst, J., Coleman, S., Stumpel, J. E., Azouz, A. B., Diamond, D., Schenning, A. P. H. J. Molecular Design of Light-Responsive Hydrogels, For in Situ Generation of Fast and Reversible Valves for Microfluidic Applications. *Chem. Mater.* **2015**, 27, 5925-5931.
7. Frances, W., Dunne, A., Delaney, C., Florea, L., Diamond, D., Spiropyran based hydrogels actuators—Walking in the light. *Sens. Actuators, B* **2017**, 250, 608–616
8. Jones, C. D., Lyon, A. Photothermal Patterning of Microgel/Gold Nanoparticle Composite Colloidal Crystals. *J. Am. Chem. Soc.* **2003**, 125, 460–465.
9. Breuer, L. et al. Hydrogels with incorporated graphene oxide as light-addressable actuator materials for cell culture environments in lab-on-chip systems *Phys. Status Solidi A*. **2016**, 213, 1520–1525
10. Greene, A. F. Danielson, M. K. Delawder, A. O. Liles, K. P. Li, X. Natraj, A. Wellen, A. Barnes, J. C. Redox-Responsive Artificial Molecular Muscles: Reversible Radical-Based Self-Assembly for Actuating Hydrogels. *Chem Mater.*, **2017**, 29 (21), 9498–9508.
11. Adamson, A. W., Demas, J. N. New photosensitizer. Tris(2,2'-bipyridine)ruthenium(II) chloride. *J. Am. Chem. Soc.* **1971** 93 (7), 1800–1801.
12. Sastre, F., Bouzidi, Y., Fornes, V., Garcia, H. Visible-light hydrogen generation using as photocatalysts layered titanates incorporating in the intergallery space ruthenium tris(bipyridyl) and methyl viologen. *J. Colloid Interface Sci.* **2010**, 346, 172–177.
13. Balamurugan, A., Reddy, M. L. P., Jayakannan, M.  $\pi$ -Conjugated polymer-Eu<sup>3+</sup> complexes: versatile luminescent molecular probes for temperature sensing *J. Mater. Chem. A* **2013**, 1, 2256–2266.
14. Eising, S., Lelivelt, F., Bongers, K. M. Vinylboronic Acids as Fast Reacting, Synthetically Accessible, and Stable Bioorthogonal Reactants in the Carboni-Lindsey Reaction. *Chem. Int. Ed. A* **2016**, 55 (40), 12243–12247.
15. Zhou, C., Truong, V., Que, Y., Lithgow, T., Fu, G., Forsythe, J. S. Antibacterial poly(ethylene glycol) hydrogels from combined epoxy-amine and thiol-ene click reaction *Polym. Sci., Part A: Polym. Chem.* **2016**, 54, 656–667.
16. Yao, F., Xu, L., Fu, G.-D., Lin, B. Sliding-Graft Interpenetrating Polymer Networks from Simultaneous “Click Chemistry” and Atom Transfer Radical Polymerization. *Macromolecules* **2010**, 43, 9761–9770
17. ABI LED Aquarium Light Bulb from Amazon [Webpage] [cited 6 December 2018], source of lightbulb used for photoredox actuation, contains emission spectrum. Available from [https://www.amazon.com/ABI-Aquarium-Light-White-PAR38/dp/B073V64KC9/ref=sr\\_1\\_3?ie=UTF8&qid=1544119524&sr=8-3&keywords=abi+led+aquarium+light+bulb](https://www.amazon.com/ABI-Aquarium-Light-White-PAR38/dp/B073V64KC9/ref=sr_1_3?ie=UTF8&qid=1544119524&sr=8-3&keywords=abi+led+aquarium+light+bulb)

# **Chapter 4: A Redox-Responsive Reversible Phottopatterned Material Produced using Free-Radical Polymerization**

This chapter is based on research that is currently unpublished.

Viologens are a group of redox-active molecules that are capable of undergoing molecular self-recognition when reduced to the radical-cation. This molecular dimerization had been used previously to actuate soft materials using both chemical and photo-chemical reduction sources. In this study, a new design strategy utilizing free-radical polymerization (FRP) is implemented to create a three-dimensional polymer network composed of mainly hydroxyethyl acrylate (HEA) with incorporation of 0.2-5 wt % electroactive oligoviologen **2V<sup>2+</sup>-St** as a crosslinker. The kinetic and mechanical properties of these hydrogels were evaluated alongside a HEA hydrogel with a poly(ethylene glycol) (PEG) crosslinker.

## **4.1 Introduction**

As has been previously shown, sequence-defined oligoviologens with glycol spacers can be incorporated into soft three-dimensional materials in order to produce actuation and work in response to a reductive stimuli.<sup>1,3</sup> This material is capable of actuating due to a multitude of factors: loss of counteranions and electrostatic repulsion and reduction in mesh size. This hydrogel has been shown to function in response to both chemical and photo-chemical reduction sources, in the form of sodium dithionite (Na<sub>2</sub>S<sub>2</sub>O<sub>4</sub>)<sup>1</sup> and from a ruthenium-based photocatalyst, tris (2,2'-bipyridine) ruthenium (II) chloride [Ru(bpy)<sub>3</sub>]<sup>2+</sup>.<sup>3</sup> Each of these hydrogels were composed primarily of PEG in the bulk material, and was polymerized using copper-alkyne

“click” chemistry. While capable of producing polymers with very precise crosslinking density, the crosslinking density cannot be easily varied. Additionally, we observed via IR spectroscopy that the click reaction to form the hydrogel did not go to completion, with many dangling ends during gel formation, presumably affecting the copper’s ability to diffuse through the network, causing incomplete integration of the polymer chains into the network. Therefore, we sought to utilize a new method of polymerizing a hydrogel network, and modify the oligoviologen accordingly, which would allow easier modification of the crosslinking density and open up a wider variety of possible monomers that could be polymerized and crosslinked.

FRP is one of the most common methods of polymerizing a hydrogel network.<sup>4-6</sup> In FRP, monomers with acrylate functional groups, usually with at least one monomer having multiple acrylates to function as a crosslinker, are mixed in a solution with a radical initiator. This radical initiator is sensitive to an external stimuli, usually heat<sup>6</sup> or UV radiation,<sup>4</sup> which then causes the initiator to break a covalent bond. The fragments of the initiator then begin propagating, reacting with vinyl groups and growing the polymer. FRP was chosen as the best means of polymerization due to its ease of use and the lack of a need to control the polymerization. To that end, our oligoviologen chain,  $2V^{2+}$  was functionalized with a styrene to allow it to be polymerized into the hydrogel network (Fig. 4.1).

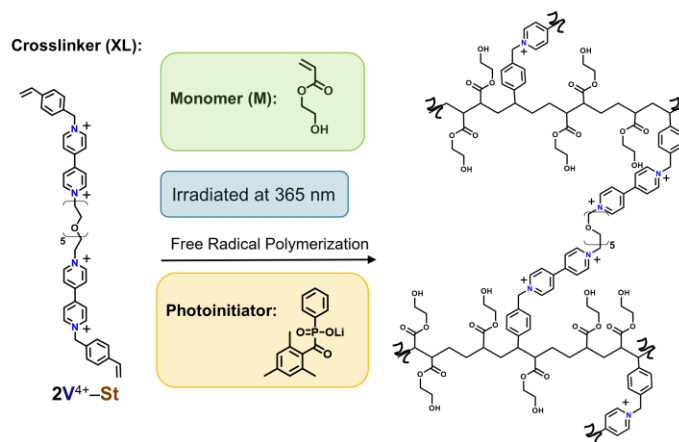


Figure 4.1 Scheme for the integration of oligoviologens crosslinker into a HEA-based polymer network.

## 4.2 Material Synthesis and Gelation Protocols

All reagents for both synthesis and gelation were purchased from commercial suppliers and used without further purification unless stated otherwise. The protocol for the synthesis of  $2V^{2+} \bullet 2Tos$  was followed as reported previously.<sup>1</sup> All photochemical reductions of oligoviologen-containing hydrogels were performed under an inert atmosphere of UHP nitrogen in either a glovebox or glovebag to prevent re-oxidation. UV irradiation for the purpose of photoinitiation was done using an Analytikjena UVP UVGL-15 using the 365 nm half (4 Watt / 0.16 Amp). Photochemical experiments were performed using a Hampton Bay desk lamps with ABI LED Aquarium Light Bulbs (12 Watt / 740 Lumens). Frequency sweep (1.0% strain, 0.1 to 100 rad s<sup>-1</sup>) and strain sweep (10 rad s<sup>-1</sup>, 0–200% strain) rheology experiments were carried out using a TA AR-G2 oscillatory shear rheometer with a 20 mm smooth geometry.

### 4.2.1 Synthesis of $2V^{4+}-St$

Dimer viologen  $2V^{2+} \bullet 2Tos$  (1 eq) and vinyl-benzyl chloride (20 eq) were dissolved in MeCN, 6 ml per 100 mg of  $2V^{2+} \bullet 2Tos$  (Fig. 4.2). The solution was then transferred to a round bottom flask equipped with a reflux condenser. The vessel was heated to 60 °C and allowed to stir for 24 h. After 24 h, the mixture was allowed to cool to RT. If there was any solid formed, MeOH was

added in 1 ml intervals until all solid is fully dissolved. The solution was then evenly distributed into two centrifuge tubes and PhMe added until the tubes were full. The tubes were centrifuged at 4490 rpm at  $-10^{\circ}\text{C}$  for 30 min. The product,  $2\text{V}^{4+}\text{-St}$ , will precipitate out as an oily-brown/black solid.  $^1\text{H}$  NMR (300 MHz, DMSO):  $\delta = 9.61(\text{d}, 4\text{H}), 9.37(\text{d}, 4\text{H}), 7.63(\text{d}, 4\text{H}), 7.56(\text{d}, 4\text{H}), 7.45(\text{d}, 4\text{H}), 7.09(\text{d}, 4\text{H}), 6.75(\text{dd}, 2\text{H}), 6.0(\text{s}, 4\text{H}), 5.89(\text{d}, 2\text{H}), 5.32(\text{d}, 2\text{H}), 4.91(\text{s}, 4\text{H}), 3.42(\text{m}, 14\text{H}), 2.25(\text{s}, 6\text{H})$ .

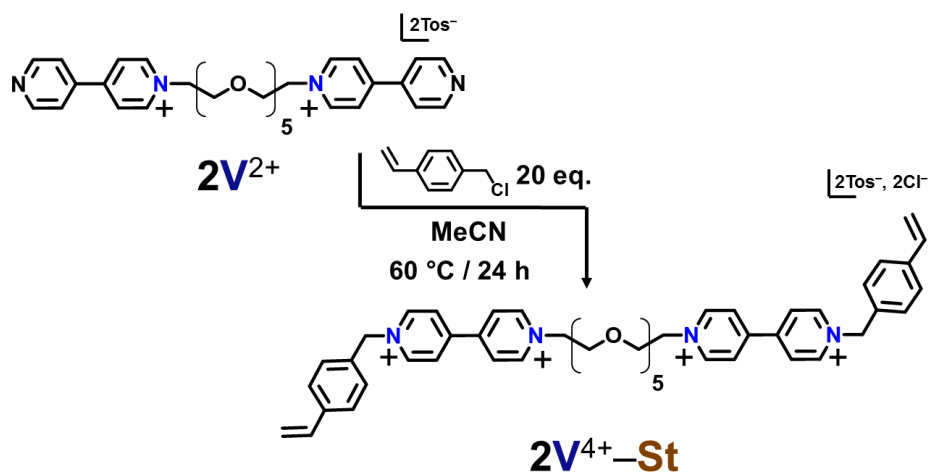


Figure 4.2 Synthesis of  $2\text{V}^{4+}\text{-St}$

#### 4.2.2 General Protocol for HEA-based Viologen-Containing Hydrogels

The reagents for polymerization (Table. 4.1) were brought into the  $\text{N}_2$ -glovebox with HEA and  $\text{H}_2\text{O}$  degassed and  $\text{O}_2$  free. All reagents, where LAP is the UV sensitive photo-initiator lithium phenyl-2,4,6-trimethylbenzoylphosphinate, were then mixed in 1.107 ml deionized (DI)  $\text{H}_2\text{O}$  and vortexed for 10–15 seconds to ensure even mixing. The entire solution was then plated into a 2.5 cm round mold and exposed to 365 nm light for 15 min. The cured hydrogels were then carefully removed from the gel mold using a spatula. Note that the gels can be incredibly difficult to remove, slowly working at the walls of the mold then lifting portions of the gel at a time until the entire gel is loose and can be easily moved. The gel was then soaked in deionized  $\text{H}_2\text{O}$  for 24 hrs.



Wt % Crosslinker	0.214%	0.431%	0.875%	1.809%	3.879%	5.000%
Mol % Crosslinker	0.021%	0.042%	0.085%	0.177%	0.387%	0.504%
HEA (mg)	442.2	437.7	428.8	410.9	375.2	357.8
2V <sup>4+</sup> -St (mg)	0.9	1.9	3.8	7.6	15.2	18.8
LAP (mg)	0.4	0.4	0.4	0.4	0.4	0.4
H <sub>2</sub> O (ml)	1.107	1.107	1.107	1.107	1.107	1.107
Total mass (mg)	443.5	440.0	432.9	418.9	390.7	377.0
Total mmoles	3.80988	3.77220	3.69684	3.54613	3.24471	3.09785
mmoles of XL	0.00078	0.00157	0.00314	0.00627	0.01254	0.01560
Wt by Vol %	40.063	39.745	39.110	37.838	35.295	34.056

Table 4.1 The amounts of each material used to fabricate viologen-containing hydrogels.

### 4.2.3 General Procedure Chemical Actuation of Hydrogels

All hydrogels were taken in their fully expanded form and placed in degassed DI water in a covered petri dish in the inert atmosphere of N<sub>2</sub> inside of a glovebag for at least 24 hrs. The water was then removed from the petri dish and 1 M Na<sub>2</sub>S<sub>2</sub>O<sub>4</sub> was added until the gel was submerged. An immediate color change to deep purple occurred upon addition of the chemical reductant. Time points were taken every 5 minutes for the first hour, then every 20 min until 3 hrs had passed. The gels were then punched with a 20 mm punch and tested for mechanical properties using oscillatory rheology (4.3.2).

### 4.2.4 General Procedure for Photo Patterning of Viologen Hydrogels

All hydrogels were taken into an inert atmosphere N<sub>2</sub> glovebox and soaked in a petri dish with a degassed “photoredox” solution containing [Ru(bpy)<sub>3</sub>]Cl<sub>2</sub> (0.15 mM) and TEOA (3.0 mM) for at least 12 hours. The photoredox solution was then removed and a photomask made of electrical tape applied to the bottom of the petri dish (Fig. 4.3). Hydrogel was irradiated with a 450 nm blue light source described above through the photomask from the bottom for 30 min.

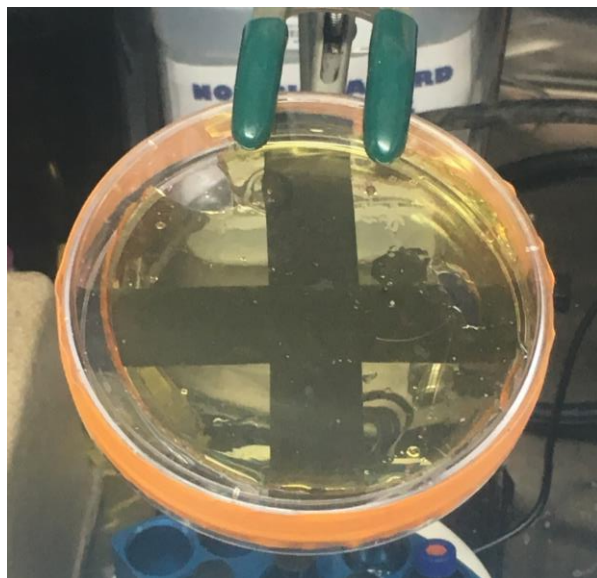


Fig. 4.3 Photo patterning experimental setup.

## 4.3 Hydrogel Characterization

### 4.3.1 Kinetic Properties of HEA-based Hydrogel Actuators

Kinetic time points are shown in Fig. 4.4 and were taken in accordance with subsection 4.2.3.

0.213, 0.430, and 0.874 weight % all have the same starting volumes (left) and contract at a rates that are not statistically significant. Thus, it can be said that at this amount of viologens no significant impact was observed on the material. However, at 1.806 weight % of crosslinker, the starting volume can be seen to increase, while sharing a similar rate of actuation to those that have lower amounts of viologen-based viologen. It is at 3.872 wt % that the largest change is seen, with a starting volume over double that of 0.213 wt %. The 5 wt % crosslinker had the largest volume increase. The higher crosslinker wt %, 3.872 and 5, are also the only hydrogel variants that display accelerated kinetics (4.4 right). While the lower four wt % compositions share roughly the same relative volume loss, after 40 minutes the 3.872 wt % hydrogels will have already lost over 50 % of its relative size, ending at ~30% after 3 hrs, indicating there is a threshold that needs to be overcome before viologen content begins to have a sizeable impact on

performance: 1.806 wt % to observe volume increases in swollen hydrogels, and 3.872 wt % crosslinked hydrogels to obtain an increase in kinetic performance.

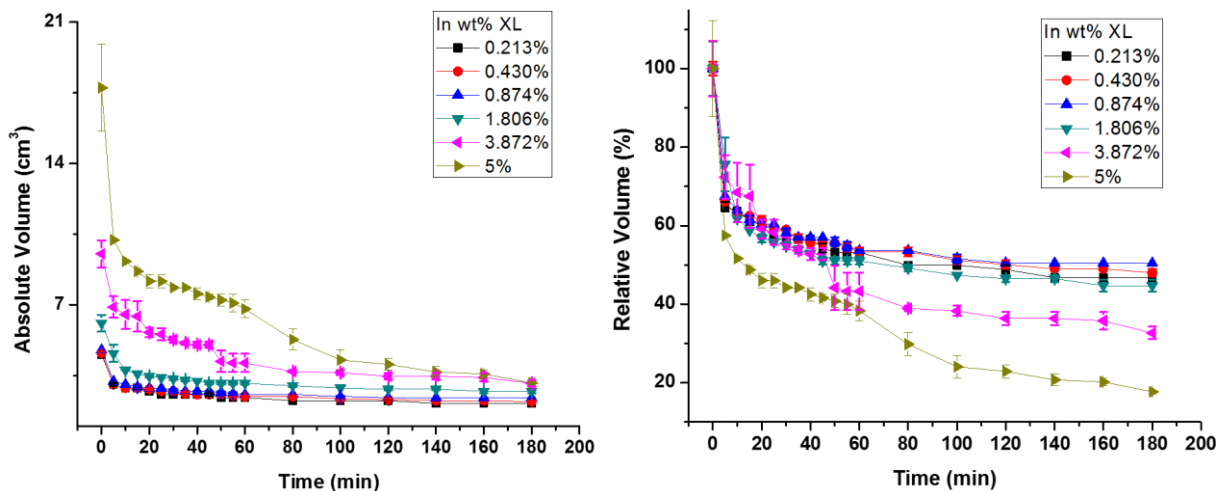


Figure 4.4 Kinetic plots of actuation out of total (left) and relative (right) volumes.

### 4.3.2 Mechanical Properties of HEA-based Hydrogel Actuators

The mechanical characteristics of the viologen-containing hydrogels shares certain trends with the kinetic data. The three lowest viologen-containing gels, 0.213, 0.430, and 0.874 wt % crosslinker, all share statistically insignificant data trends; they are also the set of hydrogels with the smallest starting volumes (Fig. 4.5 left). The hydrogels containing 1.806, 3.872, and 5 wt % crosslinker, each have progressively lower  $G'$  values in an inverse relationship of their starting volume, at least for the contracted mechanical values. Interestingly, the 1.806 wt % crosslinked hydrogel is at  $\sim 6000$  Pa along with the other, lower viologen-containing gels, with only the 3.872 and 5 wt % crosslinker-based hydrogel was significantly lower, at less than 3000 Pa (Fig. 4.5 right) in the swollen, oxidized state.

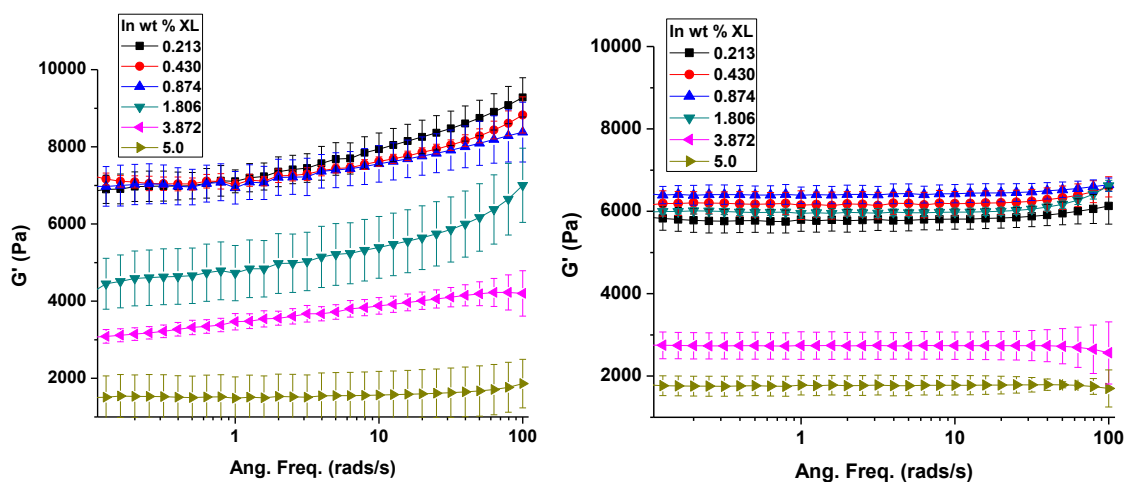


Figure 4.5 Plot of frequency sweep from 0.1 to 100 rad s<sup>-1</sup> with strain set to 1%. (Left) is the contracted hydrogels, while (right) is the swollen hydrogels.

### 4.3.3 Photo Patterned Hydrogels

Using the same “photoredox” solution and procedure in 4.2.4, gels were photo patterned using strips of black electrical tape on the bottom of the plastic petri dishes. The hydrogels (Fig. 4.6) had clear and distinct separation between what was and was not exposed to the blue light source, with the dark purple areas what was exposed and the yellow not. This indicates that the mobility inside the hydrogel is not sufficient for a reduction source to be activated and then transfer to a non-irradiated area of the gel, allowing for specific and precise photopatterning. The photomasking was reversible upon exposure to atmospheric O<sub>2</sub>, and was able to be cycled between different patterns.

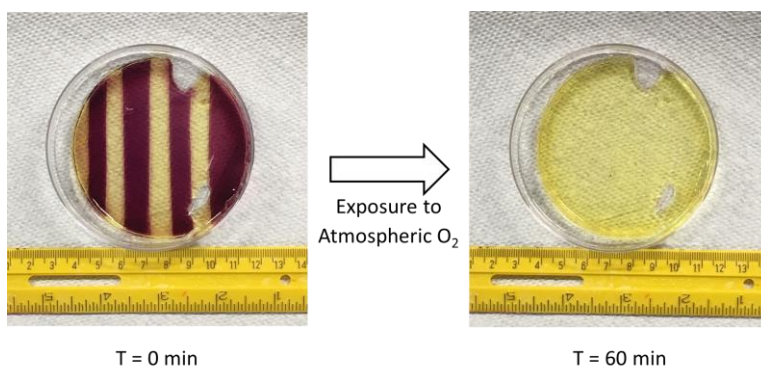


Figure 4.6 Photo pattern disappearing from hydrogel as viologens are reoxidized and loose color. Yellow color is from ruthenium-based photocatalyst

## 4.4 Conclusion

In this work, we describe a new method of polymerizing sequence-defined oligoviologens into a polymer network using uncontrolled free radical polymerization. This free radical polymerization was then utilized to polymerize a primarily HEA network with the styrene-endcapped viologen oligomer acting as the crosslinker. The actuation and mechanical properties of these HEA-based hydrogels was then ascertained, where once a threshold is reached, i.e., ~1 wt % viologen crosslinker ( $2V^{4+}$ -St), the volume of the swollen hydrogels increases while the stiffness of the material drops. These gels were then photopatterned, demonstrating the ability to precisely pattern the without the worry of reduction sources traveling to the non-irradiated areas of the hydrogel.

## References: Chapter 4

1. Greene, A. F.; Danielson, M. K.; Delawder, A. O.; Liles, K. P.; Li, X.; Natraj, A.; Wellen, A.; Barnes, J. C.: Redox-Responsive Artificial Molecular Muscles: Reversible Radical-Based Self-Assembly for Actuating Hydrogels. *Chem Mater.*, **2017**, *29*, 9498–9508.
2. Wang, B., Tahara, H., Sagara, T. Driving Quick and Large Amplitude Contraction of Viologen-Incorporated Poly-L-Lysine-Based Hydrogel by Reduction. *ACS Appl. Mater. Interfaces*, **2018**, *10*, 36415–36424.
3. Liles, K. P., Greene, A. F., et al. Photoredox-Based Actuation of an Artificial Molecular Muscle. *Macromol. Rapid Commun.* **2018**, *39*, 1700781.
4. Jeong, G. T. et al. Synthesis of poly(sorbitan methacrylate) hydrogel by free-radical polymerization. *Appl. Biochem Biotechnol.* **2007**, *137*, 935–946.
5. Haraguchi, K., Takada, T., Haraguchi, R. Nanocomposite Gels by Initiator-Free Photopolymerization: Role of Plasma-Treated Clay in the Synthesis and Network Formation. *ACS Appl. Nano. Mater.* **2018**, *1*, 418–425.
6. Li, Q.-F., Du, X., Jin, L., Hou, M., Wang, Z., Hao, J. highly luminescent hydrogels synthesized by covalent grafting of lanthanide complexes onto PNIPAm *via* one-pot free radical polymerization. *J. Mater. Chem. C.* **2016**, *4*, 3195–3201.

# **Chapter 5: Concluding Remarks**

Soft-materials containing oligomeric viologens with hexaethylene glycol spacers demonstrated remarkable ability to actuate materials in the presence of a reduction source. Using a PEG-based system, a hydrogel containing only 5 mol % oligoviologen was capable of contracting down to 9% of its original volume. Later, this same system was shown to actuate in response to a photochemical reductant, versus the chemical reductant used initially. Viologens were then incorporated into a hydrogel network using free radical polymerization by functionalizing them with styrene groups.

## **5.1 Mitigating Drawbacks**

What has been made apparent through multiple studies is that when more viologen is incorporated into a hydrogel, the weaker the mechanical properties become. While this can be easily correlated with an inverse relationship with the starting volume, the reason for increase in swelling is still a matter of study. While this is certainly a drawback, it is not insurmountable. There are many types of hydrogel actuators, namely those made with PNIPAm, that also exhibit poor mechanical strength. Viologen-containing hydrogels actually have an advantage in this regard, as viologens need only make up a small part of the material to be effective, and the monomer or additional crosslinkers can be used to mitigate this weakening of the material properties. Interpenetrating networks (IPNs) are in essence two separate physically entangled networks in one hydrogel, or binding a viologen-containing hydrogel to the side of another, tougher, material. The incorporation of nanoparticles or fibrous proteins are other alternatives. Both IPNs and nanoparticles are physical-based methods of stiffening materials rather than chemical-based. Needless to say, while the incorporation of viologens into hydrogels does weaken them, there an abundance of possible methods to remove this weakness.

## 5.2 Future Directions

With the use of viologens to actuate materials being new in the field, there are a multitude of directions that can be taken. In my opinion, one of the easiest is to explore alternative stimuli. Viologens are known to be reduced by an electric field, the backbone of redox-flow batteries, and would bring viologens into another potential method of actuation. The other is to improve the stiffness of the viologen hydrogels, which I discussed at length in section 5.1. The last potential direction is to explore other types of soft materials. The integration of oligoviologens into elastomers, plastics, and other types of soft materials would potentially allow viologen's unique properties to have other applications. Overall, there are a multitude of potential avenues to be explored and all new paths still to be trod.